Network pharmacology analysis of ZiShenWan for diabetic nephropathy and experimental verification of its anti-inflammatory mechanism

Xiaoyuan Guo
Dongfang Hospital Beijing University of Chinese Medicine
You Wu
Beijing University of Chinese Medicine
Chengfei Zhang
Beijing University of Chinese Medicine
Lili Wu
Beijing University of Chinese Medicine
Lingling Qin
Beijing University of Chinese Medicine
Tonghua Liu (thliu@vip.163.com)
Beijing University of Chinese Medicine

Research Article

Keywords: ZiShenWan, network pharmacology, diabetic nephropathy, inflammation

Posted Date: December 15th, 2020

DOI: https://doi.org/10.21203/rs.3.rs-127749/v1

Abstract

Background: Diabetic nephropathy (DN) is the leading cause of end-stage renal disease (ESRD). The inflammatory response plays a critical role in the process of DN. ZiShenWan (ZSW) is a classical Chinese medicinal formula with remarkable clinical therapeutic effects on DN, but its pharmacological action mechanisms remain unclear.

Methods: In this study, a network pharmacology approach was applied to investigate the pharmacological mechanism of ZSW in DN therapy. The “drug-ingredient-target” network for ZSW in DN treatment was established with Cytoscape software based on candidate active components of ZSW and targets in DN treatment obtained from databases. Gene ontology (GO) and Kyoto Encyclopedia of Genes and Genomes (KEGG) pathway enrichment analyses were performed with the key targets. Because inflammation is important in DN, the key targets and signaling pathways associated with the anti-inflammatory, renoprotective mechanism of ZSW were partially validated in db/db mice.

Results: A total of 56 active ingredients in ZSW and 166 DN-related targets were selected from databases. Various related genes and pathways participate in the inflammatory response. ZSW markedly alleviated renal injury in db/db mice by inhibiting the exaggerated release of proinflammatory cytokines such as interleukin (IL)-1β, IL-6, tumor necrosis factor -α (TNF-α), monocyte chemotactic protein-1 (MCP-1) and transforming growth factor-β1 (TGF-β1) and regulating the p38 mitogen-activated protein kinase (MAPK) and phosphoinositide 3-kinase-protein kinase B (PI3K-Akt) signaling pathways.

Conclusions: Network pharmacology analysis demonstrated that ZSW achieved therapeutic renoprotective effects in DN by alleviating the inflammatory response via regulation of multiple targets and signaling pathways.

Background

Diabetic nephropathy (DN), the most common complication in diabetes mellitus patients, is the leading cause of end-stage renal disease (ESRD) [1]. DN increases mortality and imposes a great physical and mental burden as well as an economic burden to individual families and society [2]. DN is clinically characterized by varying degrees of proteinuria, which can be partially alleviated by current therapies, such as renin-angiotensin system (RAS) inhibitors, in the early stage. However, progression accelerates after marked proteinuria appears [3, 4]. Therefore, the need to find effective strategies for the prevention and treatment of DN remains urgent.

Inflammation response is active throughout DN progression and plays a pivotal role especially in the early stage—participating in multiple pathological processes, including podocyte injury, glomerular basement membrane (GBM) thickening, mesangial cell proliferation, extracellular matrix (ECM) accumulation and epithelial-mesenchymal transition (EMT) in renal tubule epithelial cells. As it is stimulated by proinflammatory cytokines and involves numerous genes and signaling pathways,

inflammation has recently become a popular research focus in the mechanism of DN and has provided emerging targets for the development of DN therapy [5].

Traditional Chinese medicine (TCM) is a comprehensive medicinal system, and its application has gradually increased worldwide, with its superior therapeutic efficacy and minimal side effects. ZiShenWan (ZSW), alternatively called Tongguanwan, which consists of Anemarrhenae Rhizoma *(Anemarrhena asphodeloides* Bunge*.,* Zhimu*)*, Phellodendri Chinensis Cortex *(Phellodendron chinense* Schneid*.,* Huangbai*)* and Cinnamomum Cassia *(Cinnamomum cassia* Presl*,* Rougui*)*, is a classical Chinese medicinal prescription. It was first recorded in a famous ancient medicine treatise—LanShiMiZang, written by Li Gao during the Yuan Dynasty—and was described as a prescription for the treatment of wasting and thirsting syndrome, which was similar to diabetes mellitus. ZSW has been widely used for treating diabetes mellitus and its complications. A previous study indicated that ZSW exhibits various pharmacological activities, including antihyperglycemic activity. In addition, the main substances in ZSW have been identified and quantified [6]. However, because the ingredients of TCMs are diverse and the interactions of TCMs with the human body are complex, the specific molecular mechanisms by which ZSW acts on DN are unclear. Network pharmacology, as a breakthrough approach in the application of bioinformatics and systems biology to TCM, has sparked new interest and become a powerful strategy for research on TCM formulas [7].

This study aimed to investigate the therapeutic effects of ZSW on DN and examine the underlying mechanisms via a network pharmacology-based approach and to verify the anti-inflammatory mechanism via experiments in *db/db* mice. The flowchart of the study is shown in Fig. 1.

Methods

Network pharmacology analysis

Database building and prediction of potential targets

The candidate chemical ingredients of the three herbs contained in ZSW and the putative targets of these ingredients were identified with the Traditional Chinese Medicine Systems Pharmacology (TCMSP, http://lsp.nwu.edu.cn/tcmsp.php, updated on May 31, 2014) database using “Anemarrhenae Rhizoma”, “Phellodendri Chinensis Cortex” and “Cinnamomum Cassia” as the search terms [8]. The candidate active ingredients were screened by absorption, distribution, metabolism, and excretion (ADME) properties such as oral bioavailability (OB) and drug similarity (DL) [7]. OB≥30% and DL≥0.18 were used as the filtering criteria.

The known therapeutic targets acting on DN were searched and collected from databases including the Comparative Toxicogenomic Database (CTD, http://ctdbase.org/, updated on June 2, 2020) [9], Therapeutic Target Database (TTD, http://bidd.nus.edu.sg/group/cjttd/, updated on January 6, 2020) [10], DrugBank database (http://www.drugbank.ca/,version 5.1.6, released on April 22, 2020) [11], Online Mendelian Inheritance in Man (OMIM, http://www.omim.org/, updated on May 1, 2020) database [12],

Genetic Association Database (GAD, https://geneticassociationdb.nih.gov/, updated on September 1, 2014) [13], and Pharmacogenomics Knowledge Base (PharmGKB, https://www.pharmgkb.org/, updated on April 28, 2020) [14], using “diabetic nephropathy” as the search term. The type of target ID was unified to the Universal Protein Resource (UniProt, https://www.UniProt.org/, updated on October 15, 2019) database ID [15]. The potential targets in DN treatment were obtained by mapping the putative targets of the ingredients in ZSW and the known therapeutic targets in DN.

Network construction

A “herb-ingredient-target” network was constructed and visualized with Cytoscape software (version 3.7.1, http://www.cytoscape.org/, Massachusetts, USA) to explain the interactions between the candidate chemical ingredients of ZSW and their potential targets in DN treatment [16]. Nodes represent herbs, candidate chemical ingredients and potential targets; edges represent interactions among herbs, candidate chemical ingredients and potential targets.

The protein-protein interaction (PPI) network of potential targets was constructed with the STRING (https://string-db.org, updated on January 19, 2019) database [17]. The species was limited to human (*Homo sapiens*), and the medium confidence level was set at 0.700. The results of PPI network construction were imported into Cytoscape software and analyzed with the cytoHubba plugin. The core targets in the PPI network were identified.

Biological function and pathway analysis

Gene ontology (GO) enrichment analysis mainly describes the biological functions of genes, such as their activity, process and site of action, and is widely used in gene function classification. Enrichment analysis of the biological process (BP), cellular component (CC) and molecular function (MF) terms associated with potential targets was performed with the ClueGO plugin of Cytoscape software. Kyoto Encyclopedia of Genes and Genomes (KEGG) pathway enrichment analysis was used to study signaling pathways related to genes with the Database for Annotation, Visualization and Integrated Discovery (DAVID, https://david.ncifcrf.gov/, updated on May 2016) Bioinformatics Resources 6.8 tool, with $P < 0.05$ [18].

Experimental validation

Animals

Six-week-old male diabetic *db/db* (C57BLKS/J-lepr^{db}/lepr^{db}) mice and their male nondiabetic *db/m* (C57BLKS/J-lepr$^{db/+}$) littermates were purchased from the Model Animal Research Center of Nanjing University (Nanjing, China). The animals were housed under standard light (12 h light/dark cycle), temperature (24 ± 1°C), and relative humidity (55 ± 5%) conditions and fed a pelletized commercial chow diet. All procedures were performed in accordance with the guidelines approved by the Animal Experiments Ethics Committee of Beijing University of Chinese Medicine, China.

Drugs and reagents

ZSW is composed of Anemarrhenae Rhizoma, Phellodendri Chinensis Cortex and Cinnamomum Cassia at a ratio of 20:20:3 according to the traditional formula. Anemarrhenae Rhizoma and Phellodendri Chinensis Cortex were crushed for 30 min, macerated in 6 volumes of ethanol (50%, v/v), and extracted two times for 60 min each. Cinnamomum Cassia was added to the filtered ethanol extracts and macerated in 8 volumes of ethanol (50%, v/v). Reflux extraction was repeated twice. All ethanol extracts were combined and filtered. Last, the combined filtrate was concentrated using a rotary vacuum evaporator and was then lyophilized to obtain a powder. The yield of the ZSW extract was 11%. Dapagliflozin (DAPA; 10 mg tablets; AstraZeneca, Maryland, USA), a sodium–glucose cotransporter 2 (SGLT2) inhibitor that has been confirmed to have renoprotective and anti-inflammatory effects in diabetes mellitus models [19, 20], was used as a positive control.

Primary antibodies against rabbit interleukin (IL)-1β, IL-6, nephrin, phospho-p38 mitogen-activated protein kinase (p-p38 MAPK), transforming growth factor β1 (TGF-β1), α-smooth muscle actin (α-SMA) and GAPDH (glyceraldehyde-3-phosphate dehydrogenase) were obtained from Abcam (Cambridge, UK). The primary antibody against rabbit monocyte chemotactic protein 1 (MCP-1) was obtained from Proteintech (Illinois, USA). The primary antibody against rabbit phospho-protein kinase B Akt (p-Akt) was obtained from CST (Massachusetts, USA). The primary antibody against rabbit tumor necrosis factor -α (TNF-) was obtained from GeneTeX (California, USA). The primary antibody against rabbit type IV collagen (IV-C) was obtained from Affinity Biosciences (Ohio, USA). Urinary albumin enzyme-linked immunosorbent assay (ELISA) kits were obtained from Elabscience (Texas, USA).

Animal model and treatments

After acclimation to the environment for 2 weeks, *db/db* mice were randomly divided into 5 groups with 10 mice per group: the normal control (NC) group, high-dose ZSW (ZSW-H, 6.0 mg/kg) group, medium-dose ZSW (ZSW-M, 3.0 mg/kg) group, low-dose ZSW (ZSW-L, 1.5 mg/kg) group and DAPA (1.0 mg/kg) group. ZSW and DAPA were dissolved in deionized water for oral gavage once daily at the doses mentioned above. Mice in the NC group and *db/m* mice received only an equivalent volume of deionized water over the same treatment period. Mice had access to food and water ad libitum. The treatment duration was 12 weeks.

Sample collection

Samples for fasting blood glucose (FBG) measurement were collected by tail vein bleeding, and FBG was measured every 2 weeks. Mice were housed in individual metabolic cages for urine sample collection every 4 weeks. At the end of the 12th week of treatment, blood samples were collected by retro-orbital bleeding, and all mice were then euthanized and sacrificed. Renal tissue samples were harvested and divided into two parts. One part was fixed with 4% paraformaldehyde and stored at 4°C for section preparation, and the other part was stored at -80°C for Western blot (WB) and real-time quantitative polymerase chain reaction *(RT-qPCR)* analyses.

Blood and urine examination

Serum and urinary creatinine (CRE) and blood urea nitrogen (BUN) were measured in an automatic biochemical analyzer (Xinrui, Guangdong, China). Urinary albumin excretion was evaluated by the ratio of the urinary albumin concentration to the CRE concentration (ACR, μg/mg). The urinary albumin concentration was measured with ELISA kits in accordance with the manufacturer's instructions.

Renal histologic analysis

Renal tissue samples fixed with 4% paraformaldehyde were dehydrated through an alcohol concentration gradient and were then cleared in xylene, embedded in paraffin, and finally sliced into 3 μm thick sections. The sections were stained with hematoxylin and eosin (HE), periodic acid-Schiff (PAS) and Masson trichrome and were then examined by light microscopy for histopathological diagnosis. For transmission electron microscopy (TEM) observation, renal cortical tissues were sectioned at 1 mm, fixed with 3% glutaraldehyde, postfixed in 1% osmium tetroxide, dehydrated through a graded alcohol series and embedded in Epon 812 epoxy. Ultrathin sections (60 nm) were sliced with an ultramicrotome (RMC-Boeckeler Instruments, Arizona, USA) and were then stained with uranyl acetate and lead citrate. The sections were examined under an electron microscope (FEI Tecnai Spirit, Ohio, USA) at 6000× magnification.

Immunohistochemical (IHC) analysis

Sections (3 μm) of paraffin-embedded renal tissue were deparaffinized and rehydrated and were then incubated with 3% H_2O_2 for 10 min to quench endogenous peroxidase activity. The sections were then incubated overnight at 4°C with diluted primary antibodies against nephrin, IV-C and α-SMA (1:4000 dilution). Images were analyzed using Image-Pro Plus 6.0 software (Media Cybernetics, Maryland, USA), and staining values were expressed as the positive staining rates.

WB analysis

Total protein from renal tissues was extracted with ice-cold RIPA lysis buffer (Beyotime, Shanghai, China). The lysate was centrifuged at 10,000 × g for 15 min at 4°C. The protein concentrations were determined with a BCA Protein Assay Kit (Solarbio, Beijing, China). Equal amounts of protein were separated by SDS-PAGE and transferred to PVDF membranes (Millipore, Massachusetts, USA). Membranes were blocked in 5% nonfat milk at room temperature for 1 h and were then incubated with primary antibodies against IL-1β, IL-6, nephrin, p-Akt, TGF-β1 (all at a 1:1000 dilution), IV-C, MCP-1, p-p38 MAPK, TNF-α (all at a 1:500 dilution), α-SMA (1:100 dilution) and GAPDH (1:5000 dilution) overnight at 4°C and were then washed. After incubation with the appropriate secondary antibodies (1:1000 dilution) for 1 h at room temperature, target protein bands were detected with enhanced chemiluminescence substrate (Solarbio, Beijing, China). Each WB analysis was performed three times. Semiquantitative analysis was performed using ImageJ software (National Institutes of Health, Maryland, USA).

RT-qPCR

Total RNA from renal tissues was extracted using TRIzol reagent (Invitrogen, CA, USA) according to the manufacturer's instructions. RNA (0.2 μg) was reverse transcribed into cDNA using a SuperScript III reverse transcription reagent kit (Invitrogen, CA, USA), and equal amounts of the reverse transcription products were subjected to PCR amplification. Real-time PCR was performed in a StepOne Software Real-Time PCR system (Applied Biosystems, CA, USA).β-Actin was amplified in a parallel reaction as an internal quantitative control. The thermal cycling program used for PCR was as follows: 95°C for 10 s, followed by 40 cycles at 58°C for 20 s, 72°C for 20 s and 95°C for 5 min. The amplification curve and melting curve for real-time fluorescence quantitative PCR were performed at the end of the reaction. The cycle threshold (Ct) values were obtained for each sample well. The Ct value of β-actin in the same sample was taken as the internal normalization parameter, and relative quantitative expression levels were calculated by the $2^{-\Delta\Delta Ct}$ method. Each group was analyzed in triplicate. The primer sequences used for mouse mRNA detection are listed in Table 1.

Table 1 Primers sequences of RT-qPCR

Target	Forward (5' to 3')	Reverse (5' to 3')
IV-C	TGAACAAGCTCTGGAGTGGGTACAG	GTACAGGAAAGGCATGGTGCTGAAG
α-SMA	GGAAAAGATCTGGCACCACTC	TTTCTCCCGGTTGGCCTT
Akt	ATGAACGACGTAGCCATTGTG	TTGTAGCCAATAAAGGTGCCAT
IL-1β	GTGAAATGCCACCTTTTGACA	GATTTGAAGCTGGATGCTCT
IL-6	CTTCCATCCAGTTGCCTT	CTGTGAAGTCTCCTCTCCG
MCP-1	CTGCTGCTACTCATTCACCA	CTTCTTTGGGACACCTGC
nephrin	TCTGGGTCCAAACCCTAAGATT	TCAATAAGCAGGTGGAACTCAC
p38 MAPK	TGACCCTTATGACCAGTCCTTT	GTCAGGCTCTTCCACTCATCTAT
TGF-β1	CTTCAATACGTCAGACATTCGGG	GTAACGCCAGGAATTGTTGCTA
TNF-α	TTCCCAAATGGCCTCCCTC	TCCAGCTGCTCCTCCACT
β-Actin	CCCATCTATGAGGGTTACGC	TTTAATGTCACGCACGATTTC

Statistical analysis

All data are shown as the mean ± standard deviation (SD) values. Data were analyzed with Statistical Product and Service Solutions software 22.0 (Illinois, USA). Analysis of variance (ANOVA) was carried out to determine statistical significance for comparisons among multiple parameters. The least significant difference (LSD) test was performed under the assumption of equal variances; otherwise, Dunnett's T3 test was applied for data with unequal variances. Statistical significance was established at $P < 0.05$ or $P < 0.01$.

Results

Chemical ingredients in the candidates

A total of 56 chemical ingredients in the three herbal medicines in ZSW were screened in TCMSP by ADME parameters (OB ≥ 30% and DL ≥ 0.18): 15 ingredients in Anemarrhenae Rhizoma, 36 ingredients in Phellodendri Chinensis Cortex and 10 ingredients in Cinnamomum Cassia. Among the screened compounds, stigmasterol was the common constituent of the three herbal medicines. Kaempferol was found in both Anemarrhenae Rhizoma and Cinnamomum Cassia, while quercetin was found in both Phellodendri Chinensis Cortex and Cinnamomum Cassia.

Prediction of potential targets

The putative targets of the candidate ingredients in ZSW were identified in the TCMSP database: 94 for Anemarrhenae Rhizoma, 137 for Phellodendri Chinensis Cortex and 142 for Cinnamomum Cassia. In total, 18824 known therapeutic targets for DN were identified in the CTD, the TTD, DrugBank, OMIM, the GAD and PharmGKB. Finally, 166 potential treatment targets in DN were obtained.

Network construction

The “herb-ingredient-target” interaction network of ZSW for DN treatment was constructed with Cytoscape software and contained 220 nodes and 1093 edges (Fig. 2). The average degree value in the network was 9.93. Among the candidate chemical ingredients, 31 had a degree larger than the average degree value listed in Table 2.

Table 2 General information of the main active ingredients of ZSW

Herb	Ingredient name	Degree
Phellodendri Chinensis Cortex	quercetin	86
Cinnamomum Cassia		
Cinnamomum Cassia	epicatechin	54
Anemarrhenae Rhizoma	kaempferol	54
Cinnamomum Cassia		
Cinnamomum Cassia	cinnamyl acetate	54
Phellodendri Chinensis Cortex	Isocorypalmine	53
Phellodendri Chinensis Cortex	beta-sitosterol	49
Phellodendri Chinensis Cortex	(S)-Canadine	48
Phellodendri Chinensis Cortex	Cavidine	45
Anemarrhenae Rhizoma	stigmasterol	44
Phellodendri Chinrnsis Cortex		
Cinnamomum Cassia		
Phellodendri Chinensis Cortex	Fumarine	44
Anemarrhenae Rhizoma	Anhydroicaritin	39
Phellodendri Chinensis Cortex	Dehydrotanshinone II A	30
Phellodendri Chinensis Cortex	rutaecarpine	30
Phellodendri Chinensis Cortex	berberine	29
Phellodendri Chinensis Cortex	palmatine	29
Cinnamomum Cassia	Procyanidin B1	28
Cinnamomum Cassia	isoliquiritigenin	26
Phellodendri Chinensis	berberrubine	26

Cortex			
Phellodendri	Chinensis	thalifendine	26
Cortex			
Phellodendri	Chinensis	phellamurin_qt	25
Cortex			
Phellodendri	Chinensis	Phellopterin	24
Cortex			
Phellodendri	Chinensis	coptisine	20
Cortex			
Phellodendri	Chinensis	Chelerythrine	20
Cortex			
Anemarrhenae Rhizoma		(Z)-3-(4-hydroxy-3-methoxy-phenyl)-N-[2-(4-hydroxyphenyl)ethyl]acrylamide	18
Anemarrhenae Rhizoma		coumaroyltyramine	18
Phellodendri	Chinensis	Skimmianin	17
Cortex			
Anemarrhenae Rhizoma		Hippeastrine	16
Phellodendri	Chinensis	Phellavin_qt	15
Cortex			
Phellodendri	Chinensis	Worenine	15
Cortex			
Anemarrhenae Rhizoma		diosgenin	14
Cinnamomum Cassia		cinnamic acid	11

The PPI network was constructed with the STRING database and the Cytoscape cytoHubba plugin with a medium confidence level of 0.700. A total of 154 targets were screened and analyzed (Fig. 3). The average degree value in the PPI network was calculated to be 10.59. Sixty selected core targets had a degree value larger than the average value. The top 20 core targets are listed in Table 3.

Table 3 Core targets in PPI network of ZiShenWan in treating DN

Gene name	Target name	Degree
IL6	Interleukin-6	41
MAPK1	Mitogen-activated protein kinase 1	41
JUN	Transcription factor AP-1	40
APP	Amyloid-beta precursor protein	38
TP53	Cellular tumor antigen p53	38
EGF	Pro-epidermal growth factor	38
MAPK8	Mitogen-activated protein kinase 8	37
VEGFA	Vascular endothelial growth factor A	37
TNF	Tumor necrosis factor	33
MAPK3	Mitogen-activated protein kinase 3	33
EGFR	Epidermal growth factor receptor	32
PTGS2	Prostaglandin G/H synthase 2	28
IL1B	Interleukin-1 beta	27
ESR1	Estrogen receptor	26
SAA1	Serum amyloid A-1 protein	24
F2	Prothrombin	22
AR	Androgen receptor	22
MAPK14	Mitogen-activated protein kinase 14	21
CCL2	C-C motif chemokine 2	20
NOS3	Nitric oxide synthase, endothelial	20

Biological function and pathway analysis

Biological function analysis of the candidate chemical ingredients in ZSW for DN treatment was carried out with the Cytoscape ClueGO plugin, with $P < 0.05$. The key targets were involved in biological processes such as the G-protein coupled receptor signaling pathway, lipopolysaccharide-mediated signaling pathway, oxidation-reduction process, synaptic transmission, and cell-cell signaling (Fig. 4A). GO cell component enrichment analysis indicated that the targets were enriched mainly in the terms cell junction, synapse, ECM, GABA-A receptor complex, and cytosol (Fig. 4B). The enriched molecular function terms were mainly G-protein coupled receptor activity, GABA-A receptor activity, and activation of MAPK activity (Fig. 4C). The GO enrichment results for the top 10 terms are shown as a histogram (Fig. 4D).

Pathway enrichment analysis of DN treatment targets of ZSW f was performed with the DAVID Bioinformatics Resources 6.8 tool, and significant pathways were identified as those with $P < 0.05$. The enrichment results of the top 50 KEGG pathways are shown in a bubble chart (Fig. 5A). The core target

pathways included inflammatory reaction, advanced glycosylation end products (AGEs), cell proliferation and differentiation, endocrine resistance, nerve tissue conduction and other related pathways. The “target-top 50 pathways” network data were imported into Cytoscape software, and the network was constructed (Fig. 5B).

ZSW improved the blood sugar and renal injury biochemical index levels in db/db mice

As expected, our study showed that FBG levels were much higher in eight-week-old *db/db* mice than in *db/m* mice of the same age ($P < 0.01$). Biweekly blood glucose tests showed that as early as the second week of treatment, all doses of ZSW and DAPA significantly decreased FBG levels in *db/db* mice ($P < 0.01$). Compared to that of *db/m* mice, the urinary ACR of *db/db* mice was increased and was effectively reduced by ZSW and DAPA treatment ($P<0.01$). As the treatment duration increased, the reduction in urinary ACR increased. Both the BUN and serum CRE levels were higher in *db/db* mice than in *db/m* mice ($P < 0.01$). DAPA and all doses of ZSW significantly blunted the increases in BUN and serum CRE ($P < 0.01$). These results are shown in Fig. 6.

ZSW ameliorated pathological damage and regulated biomarkers of renal tissues in db/db mice

HE, PAS and Masson staining showed glomerular hypertrophy, GBM thickening, mesangial matrix expansion and tubular inflammation in *db/db* mice. However, these injuries were attenuated to varying extents by DAPA and ZSW treatment. All these changes were significantly confirmed by TEM observation (as shown in Fig. 7). As a marker of podocytes, nephrin expression was markedly lower in the renal tissue of *db/db* mice than in the renal tissue of *db/m* mice. This reduction in nephrin expression was reversed by ZSW and DAPA treatment. The increased IV-C level in *db/db* mice indicated ECM proliferation in renal tissues, and the IV-C level was decreased by ZSW and DAPA treatment. The expression level of α-SMA, a marker of fibrosis, was higher in *db/db* mice than in *db/m* mice, and α-SMA expression was inhibited by DAPA and ZSW treatment. All these findings were determined by IHC analysis ($P < 0.01$, as shown in Fig. 8). The protein and mRNA levels of these biomarkers were subsequently measured by WB analysis and RT-qPCR ($P < 0.01$, as shown in Fig. 9).

ZSW inhibited the expression of multiple proinflammatory cytokines in db/db mice

Compared with those in the *db/m* group, the protein levels of proinflammatory cytokines, including IL-1β, IL-6, TNF-α, MCP-1, and TGF-β1, were significantly increased in the NC group ($P < 0.01$, as shown in Fig. 10A and B), as were the mRNA levels of these cytokines ($P < 0.01$, as shown in Fig. 10C). As shown in Fig. 10, the protein and mRNA levels of the abovementioned proinflammatory cytokines were significantly reduced in *db/db* mice treated with ZSW or DAPA compared with NC mice ($P < 0.01$).

ZSW regulated the phosphoinositide 3-kinase (PI3K)-Akt and p38 MAPK signaling pathways in db/db mice

As shown in Fig. 11A and B, the levels of p-Akt and p-p38 were significantly increased in *db/db* mice compared with *db/m* mice ($P < 0.01$). Moreover, compared with those in *db/db* mice, the levels of p-Akt

and p-p38 were significantly decreased by 12 weeks of ZSW or DAPA treatment ($P < 0.01$). As shown in Fig. 11C, the mRNA levels of Akt and p38 were increased in *db/db* mice compared with *db/m* mice ($P < 0.01$) and were significantly lower in all ZSW groups and the DAPA group than in the NC group ($P < 0.01$).

Discussion

Abnormal glycolipid metabolism, inflammation, oxidative stress, AGEs, hemodynamic disorders and other factors are implicated in DN pathogenesis [21]. The abovementioned mechanisms were validated as the main mechanistic targets of ZSW in DN therapy, as supported by network pharmacology analysis. This study confirmed the multitarget and multipathway activities of ZSW in DN treatment.

Chronic low-grade inflammation exists widely in patients with diabetes mellitus and is essential for the progression of DN [22]. Notably, inflammation is attributed to glucose metabolism disorder, which leads to glucose self-oxidation and metabolic stress responses [23]. Consequently, blood glucose control is the basic principle in the prevention and treatment of DN. As a model of spontaneous diabetes, *db/db* mice exhibit increased blood glucose levels as a result of leptin receptor gene mutation and functional loss [24]. Our study demonstrated that ZSW reduced the FBG levels in *db/db* mice, suggesting a hypoglycemic effect as an underlying renoprotective and anti-inflammatory mechanism.

As they mimic many of the characteristics of early human DN, *db/db* mice are widely used in efficacy and mechanistic studies of DN therapies [25]. ZSW was validated in our current study as a potent treatment for renal injuries in *db/db* mice, with evidence of decreased urinary ACR, serum CRE and BUN. Regarding pathology, the glomerular hypertrophy, GBM thickening, mesangial expansion and matrix deposition in *db/db* mice were ameliorated to varying degrees by ZSW. In addition, the extent of tubulointerstitial injury ultimately determines the rate of attrition of renal function [26]. Vacuolar degeneration and inflammatory cell infiltration are present in tubular epithelial cells of *db/db* mice and were alleviated by ZSW in the current study.

We further evaluated the effects of ZSW on the typical marker proteins of both intrinsic renal cells and pathological processes in *db/db* mice. Nephrin maintains the functions of the renal filtration barrier. Previous studies have shown that high glucose reduces the stability of nephrin, which often leads to podocyte injury, proteinuria and renal failure [27]. We showed that ZSW reversed the reduction in nephrin expression in *db/db* mice. IV-C is physiologically expressed in the GBM. However, excessive IV-C secretion leads to the accumulation of ECM, resulting in GBM thickening and mesangial matrix expansion in DN [28], as shown in our study by Masson staining, IHC analysis and WB analysis. As expected, ZSW decreased the overexpression of IV-C. The number of myofibroblasts is inversely correlated with renal function in DN. As the putative marker of myofibroblasts, α-SMA is expressed in cells primarily located in the renal interstitium and, to a lesser extent, in glomeruli in association with mesangial proliferation [29]. In this study, α-SMA was highly expressed in *db/db* mice, while ZSW downregulated its expression. These results suggested the renoprotective effects of ZSW in DN treatment.

Cytokines are essential for mediating inflammation throughout the progression of DN. ILs are classical inflammatory factors. IL-6, encoded by the IL6 gene, promotes ECM production and mesangial cell proliferation, changes vascular permeability, and accelerates GBM thickening. IL-1β, encoded by the IL1B gene, activates and aggregates immune cells; induces the synthesis and release of other inflammatory cytokines (such as IL-6), chemokines and adhesion molecules; and amplifies the local or systemic inflammatory response. TNF-α, encoded by the TNF gene, promotes renal cell apoptosis and accelerates the development of microalbuminuria and renal fibrosis. A previous study found that the level of serum TNF-α in DN patients was significantly higher than that in patients without renal injury [30]. MCP-1, which is encoded by CCL2, is the most well-known chemokine regulator of monocytes and is upregulated in DN patients. It regulates the expression of adhesion molecules and increases and recruits monocytes to the glomerulus. Moreover, it promotes the release of inflammatory mediators such as IL-1 and IL-6, induces oxidative stress, activates proteolytic enzymes and damages endothelial cells [31]. A multifunctional cytokine that controls numerous biological processes, TGF-β1 has been widely acknowledged to be involved in the pathogenesis of DN. Overexpression of TGF-β1 induced by the diabetic milieu promotes both cell hypertrophy and ECM accumulation and induces EMT. These pathological processes eventually result in glomerular sclerosis and renal interstitial fibrosis [32]. We investigated the abovementioned cytokines as the core targets of ZSW in DN therapy by network pharmacology analysis. The regulatory role of ZSW in the protein and mRNA expression of these cytokines was verified by in vivo experiments.

MAPK is a member of the serine/threonine protein kinase family [33]. Among the four members of the MAPK family, p38 MAPK plays a critical role in inflammation. Inflammation-related cytokines can activate the p38 MAPK signaling pathway, which accelerates the progression of DN by promoting cell proliferation and ECM production [34]. The PI3K-Akt signaling pathway mediates the differentiation, proliferation, apoptosis and migration of cells. However, excessive activation of this pathway stimulated by factors such as hyperglycemia results in cell dysfunction. In DN, overactivated Akt accelerates ECM accumulation and EMT in renal tubular epithelial cells, eventually promoting the progression of glomerulosclerosis and renal interstitial fibrosis [35]. We found that both the MAPK and PI3K-Akt signaling pathways were among the top 50 KEGG pathways; moreover, the genes encoding the related targets s were the key targets of ZSW in DN treatment. In addition, ZSW was indicated to decrease the phosphoprotein and mRNA levels of p38 and Akt in *db/db* mice, indicating that ZSW exerted its therapeutic effects on DN partially by regulating the related signaling pathways.

However, this study has several limitations. Information about the early pathogenesis of DN available in databases is relatively insufficient. In addition, the in vivo experimental verification did not include all targets and pathways associated with inflammation. Moreover, the complex metabolism of herbs in the human body is still incompletely characterized and cannot be completely reflected in animal models. Thus, more therapeutic effects and mechanisms need to be explored and verified by further research.

Conclusions

In conclusion, according to network pharmacology analysis, the effective mechanisms of ZSW in DN therapy involve the regulation of targets and pathways in multiple biological processes, particularly inflammation. ZSW's anti-inflammatory activity in *db/db* mice may be mediated by inhibition of the exaggerated release of proinflammatory cytokines and regulation of the p38 MAPK and PI3K-Akt signaling pathways. ZSW might be used as a potent therapeutic agent for DN.

Abbreviations

IV-C: type IV collagen; α-SMA: α-smooth muscle actin; ACR: albumin concentration versus creatinine concentration ratio; ADME: absorption, distribution, metabolism and excretion; Akt: protein kinase B; BUN: blood urea nitrogen; CRE: creatinine; CTD: Comparative Toxicogenomic Database; DAPA: dapagliflozin; DN: diabetic nephropathy; FBG: fasting blood glucose; GAPDH: glyceraldehyde-3-phosphate dehydrogenase; GO: gene ontology; HE: hematoxylin and eosin; IHC: immunohistochemistry; IL: interleukin; KEGG: Kyoto encyclopedia of genes and genomes; MAPK: mitogen activated protein kinases; MCP-1: monocyte chemotactic protein-1; NC: normal control; OMIM: Online Mendelian Inheritance in Man; PAS: periodic acid-Schiff; PHARMGKB: Pharmacogenomics Knowledge Base; PI3K: phosphoinositide 3-kinase; PPI: protein-protein interaction; RT-qPCR: real-time quantitative polymerase chain reaction; TCMSP: Traditional Chinese Medicine Systems Pharmacology; TEM: transmission electron microscopy; TGF-β1: transforming growth factor-β1; TNF-α: tumor necrosis factor receptor-; TTD: Therapeutic Target Database; WB: Western blotting; ZSW: ZiShenWan.

Declarations

Ethics approval and consent to participate

The protocol for animal use was approved by the Animal Experiments Ethics Committee of Beijing University of Chinese Medicine. For consent to participate, not applicable.

Consent for publication

Not applicable.

Availability of data and materials

All data generated or analyzed during this study are included in this published article.

Competing interests

The authors declare that they have no competing interests.

Funding

This work was supported by the International Cooperation Project of State Administration of Traditional Chinese Medicine (No. GZYYGJ2019034). The funding body has no role in designing the study, collection, analysis, and interpretation of data and in writing the manuscript.

Authors' contributions

T-HL identified the problem and proposed the study. X-YG, YW and C-FZ designed the protocol and carried out experimentation. L-LW and L-LQ analyzed the data. T-HL and X-YG wrote this manuscript and L-LW and L-LQ revised this article. All authors read and approved the manuscript for publication.

Acknowledgements

Not applicable.

References

1. Zhang L, Long J, Jiang W, Shi Y, He X, Zhou Z, et al. Trends in chronic kidney disease in China. N Engl J Med. 2016;375:905-6.
2. Wen CP, Chang CH, Tsai MK, Lee JH, Lu PJ, Tsai SP, et al. Diabetes with early kidney involvement may shorten life expectancy by 16 years. Kidney Int. 2017;92:388-96.
3. Lewis EJ, Lewis JB. Treatment of diabetic nephropathy with angiotensin II receptor antagonist. Clin Exp Nephrol. 2003;7:1-8.
4. Gallagher H, Suckling RJ. Diabetic nephropathy: where are we on the journey from pathophysiology to treatment? Diabetes Obes Metab. 2016;18:641-7.
5. Donate-Correa J, Luis-Rodríguez D, Martín-Núñez E, Tagua VG, Hernández-Carballo C, Ferri C, et al. Inflammatory targets in diabetic nephropathy. J Clin Med. 2020;9:458.
6. Tang YH, Sun ZL, Fan MS, Li ZX, Huang CG. Anti-diabetic effects of TongGuanWan, a Chinese traditional herbal formula, in C57BL/KsJ-db/db mice. Planta Med. 2012;78:18-23.
7. Zhang GB, Li QY, Chen QL, Su SB. Network pharmacology: a new approach for chinese herbal medicine research. Evid Based Complement Alternat Med. 2013;2013:621423.
8. Ru J, Li P, Wang J, Zhou W, Li B, Huang C, et al. TCMSP: a database of systems pharmacology for drug discovery from herbal medicines. J Cheminform. 2014;6:13.
9. Davis AP, Grondin CJ, Johnson RJ, Sciaky D, McMorran R, Wiegers J, et al. The Comparative toxicogenomics database: update 2019. Nucleic Acids Res. 2019;47:D948-54.
10. Wang Y, Zhang S, Li F, Zhou Y, Zhang Y, Wang Z, et al. Therapeutic target database 2020: enriched resource for facilitating research and early development of targeted therapeutics. Nucleic Acids Res. 2020;48:D1031-41.
11. Wishart DS, Feunang YD, Guo AC, Lo EJ, Marcu A, Grant JR, et al. DrugBank 5.0: a major update to the DrugBank database for 2018. Nucleic Acids Res. 2018;46:D1074-82.

12. Hamosh A, Scott AF, Amberger JS, Bocchini CA, McKusick VA. Online mendelian inheritance in man (OMIM), a knowledgebase of human genes and genetic disorders. Nucleic Acids Res. 2005;33:D514-7.
13. Becker KG, Barnes KC, Bright TJ, Wang SA. The genetic association database. Nat Genet. 2004;36:431-2.
14. Whirl-Carrillo M, McDonagh EM, Hebert JM, Gong L, Sangkuhl K, Thorn CF, et al. Pharmacogenomics knowledge for personalized medicine. Clin Pharmacol Ther. 2012;92:414-7.
15. Morgat A, Lombardot T, Coudert E, Axelsen K, Neto TB, Gehant S, et al. Enzyme annotation in UniProtKB using Rhea. Bioinformatics. 2020;36:1896-901.
16. Otasek D, Morris JH, Bouças J, Pico AR, Demchak B. Cytoscape automation: empowering workflow-based network analysis. Genome Biol. 2019;20:185.
17. Szklarczyk D, Gable AL, Lyon D, Junge A, Wyder S, Huerta-Cepas J, et al. STRING v11: protein-protein association networks with increased coverage, supporting functional discovery in genome-wide experimental datasets. Nucleic Acids Res. 2019;47:D607-13.
18. Huang Da W, Sherman BT, Lempicki RA. Systematic and integrative analysis of large gene lists using DAVID bioinformatics resources. Nat Protoc. 2009;4:44-57.
19. Jaikumkao K, Pongchaidecha A, Chueakula N, Thongnak LO, Wanchai K, Chatsudthipong V, et al. Dapagliflozin, a sodium-glucose co-transporter-2 inhibitor, slows the progression of renal complications through the suppression of renal inflammation, endoplasmic reticulum stress and apoptosis in prediabetic rats. Diabetes Obes Metab. 2018;20:2617-26.
20. ElMahdy MK, Helal MG, Ebrahim TM. Potential anti-inflammatory effect of dapagliflozin in HCHF diet- induced fatty liver degeneration through inhibition of TNF-α, IL-1β, and IL-18 in rat liver. Int Immunopharmacol. 2020;86:106730.
21. Kanwar YS, Sun L, Xie P, Liu FY, Chen S. A glimpse of various pathogenetic mechanisms of diabetic nephropathy. Annu Rev Pathol. 2011;6:395-423.
22. Zhang J, Zhang R, Wang Y, Wu Y, Li H, Han Q, et al. Effects of neutrophil-lymphocyte ratio on renal function and histologic lesions in patients with diabetic nephropathy. Nephrology (Carlton). 2019;24:1115-21.
23. Zou LX, Sun L. Global diabetic kidney disease research from 2000 to 2017: a bibliometric analysis. Medicine (Baltimore). 2019;98:e14394.
24. Chen H, Charlat O, Tartaglia LA, Woolf EA, Weng X, Ellis SJ, et al. Evidence that the diabetes gene encodes the leptin receptor: identification of a mutation in the leptin receptor gene in db/db mice. Cell. 1996;84:491-5.
25. Sharma K, McCue P, Dunn SR. Diabetic kidney disease in the db/db mouse. Am J Physiol Renal Physiol. 2003;284:F1138-44.
26. Tang SC, Lai KN. The pathogenic role of the renal proximal tubular cell in diabetic nephropathy. Nephrol Dial Transplant. 2012;27:3049-56.

27. Tung CW, Hsu YC, Shih YH, Chang PJ, Lin CL. Glomerular mesangial cell and podocyte injuries in diabetic nephropathy. Nephrology (Carlton). 2018;23 Suppl 4:32-7.
28. Okonogi H, Nishimura M, Utsunomiya Y, Hamaguchi K, Tsuchida H, Miura Y, et al. Urinary type IV collagen excretion reflects renal morphological alterations and type IV collagen expression in patients with type 2 diabetes mellitus. Clin Nephrol. 2001;55:357-64.
29. Li J, Qu X, Bertram JF. Endothelial-myofibroblast transition contributes to the early development of diabetic renal interstitial fibrosis in streptozotocin-induced diabetic mice. Am J Pathol. 2009;175:1380-8.
30. Chen YL, Qiao YC, Xu Y, Ling W, Pan YH, Huang YC, et al. Serum TNF-α concentrations in type 2 diabetes mellitus patients and diabetic nephropathy patients: a systematic review and meta-analysis. Immunol Lett. 2017;186:52-8.
31. Park J, Ryu DR, Li JJ, Jung DS, Kwak SJ, Lee SH, et al. MCP-1/CCR2 system is involved in high glucose-induced fibronectin and type IV collagen expression in cultured mesangial cells. Am J Physiol Renal Physiol. 2008;295:F749-57.
32. Chang AS, Hathaway CK, Smithies O, Kakoki M. Transforming growth factor-β1 and diabetic nephropathy. Am J Physiol Renal Physiol. 2016;310:F689-96.
33. Cargnello M, Roux PP. Activation and function of the MAPKs and their substrates, the MAPK-activated protein kinases. Microbiol Mol Biol Rev. 2011;75:50-83.
34. Ma FY, Liu J, Nikolic-Paterson DJ. The role of stress-activated protein kinase signaling in renal pathophysiology. Braz J Med Biol Res. 2009;42:29-37.
35. Rane MJ, Song Y, Jin S, Barati MT, Wu R, Kausar H, et al. Interplay between Akt and p38 MAPK pathways in the regulation of renal tubular cell apoptosis associated with diabetic nephropathy. Am J Physiol Renal Physiol. 2010;298:F49-61.

Figures

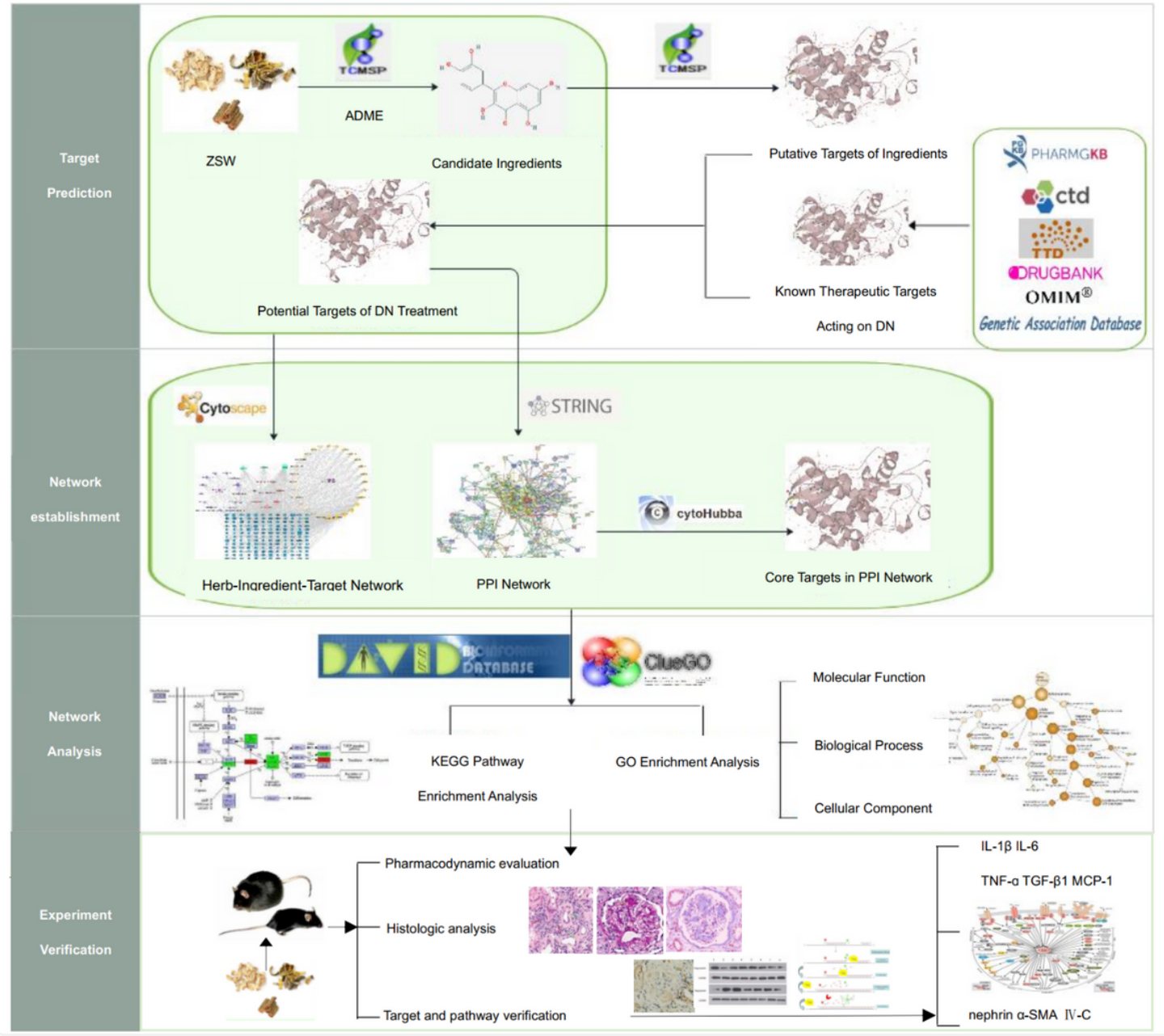

Figure 1

Flow diagram of network pharmacological analysis and experimental verification of ZSW for DN treatment.

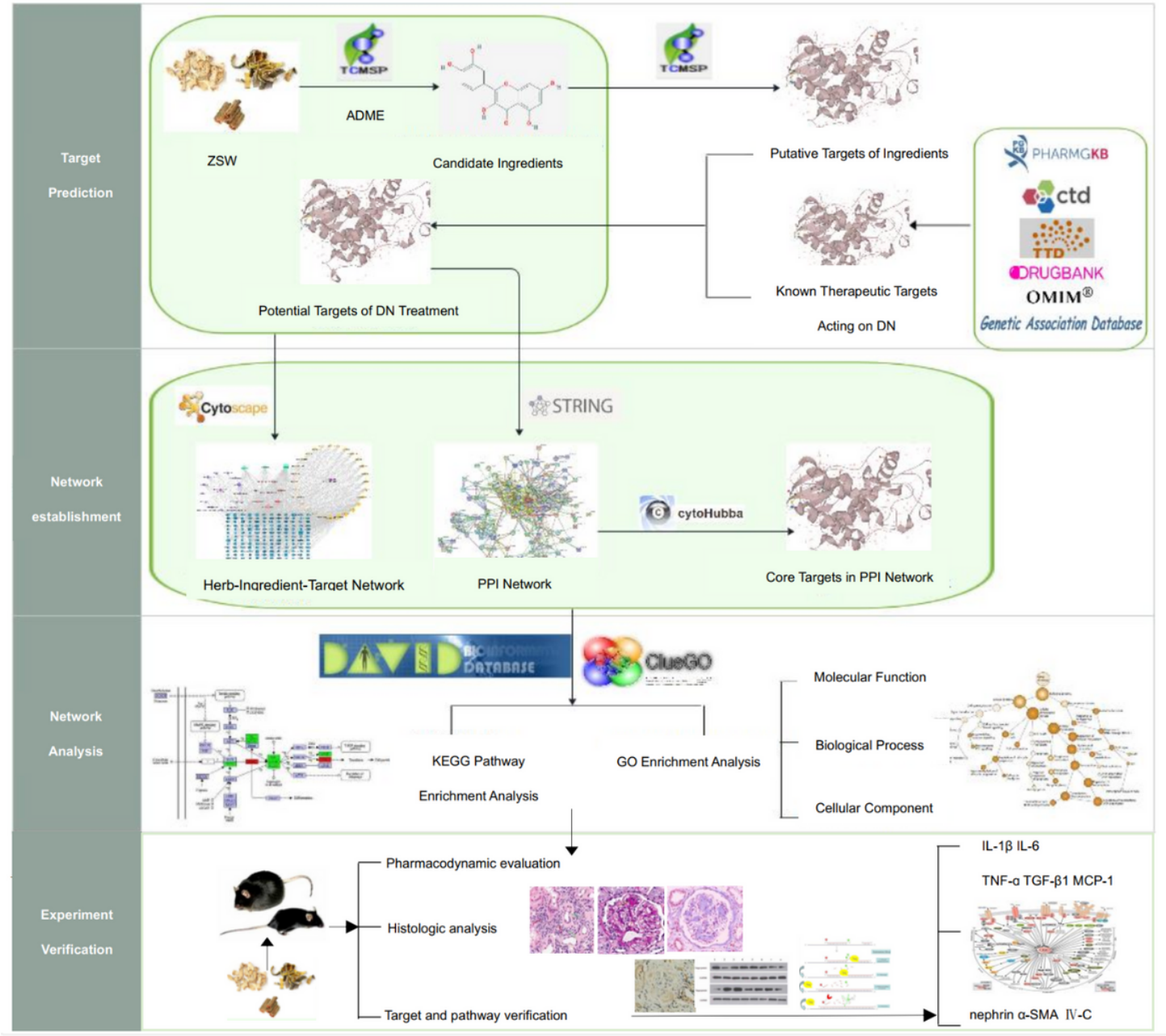

Figure 1

Flow diagram of network pharmacological analysis and experimental verification of ZSW for DN treatment.

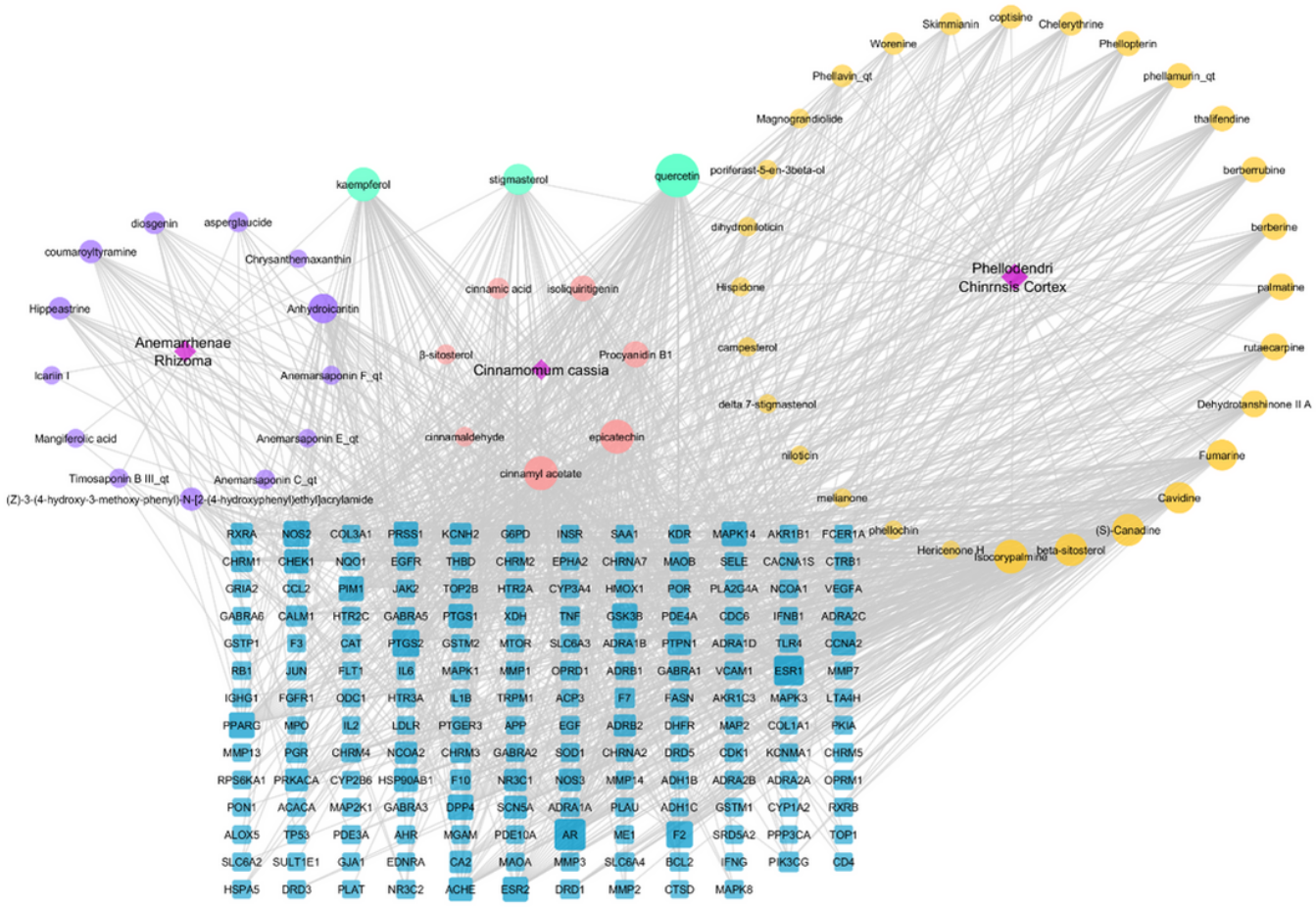

Figure 2

The “herb-ingredient-target” interaction network of ZSW for DN treatment. The purple part represents the unique active components of Anemarrhenae Rhizoma. The yellow part represents the unique active components of Phellodendri Chinensis Cortex. The pink part represents the unique active components of Cinnamomum Cassia. The blue nodes represent the target of chemical composition interaction, and each gray edge represents the interaction between compound molecules and targets.

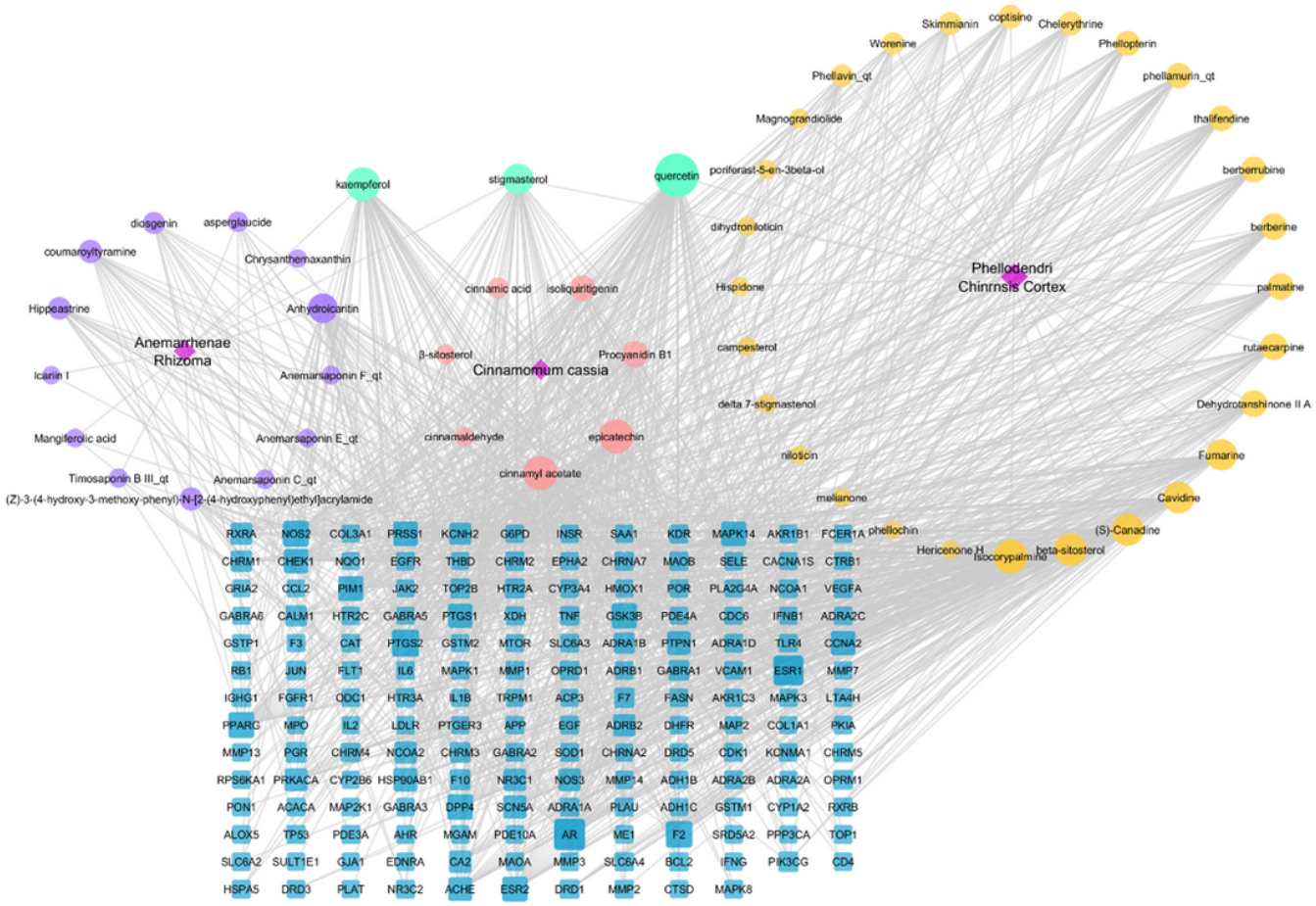

Figure 2

The “herb-ingredient-target” interaction network of ZSW for DN treatment. The purple part represents the unique active components of Anemarrhenae Rhizoma. The yellow part represents the unique active components of Phellodendri Chinensis Cortex. The pink part represents the unique active components of Cinnamomum Cassia. The blue nodes represent the target of chemical composition interaction, and each gray edge represents the interaction between compound molecules and targets.

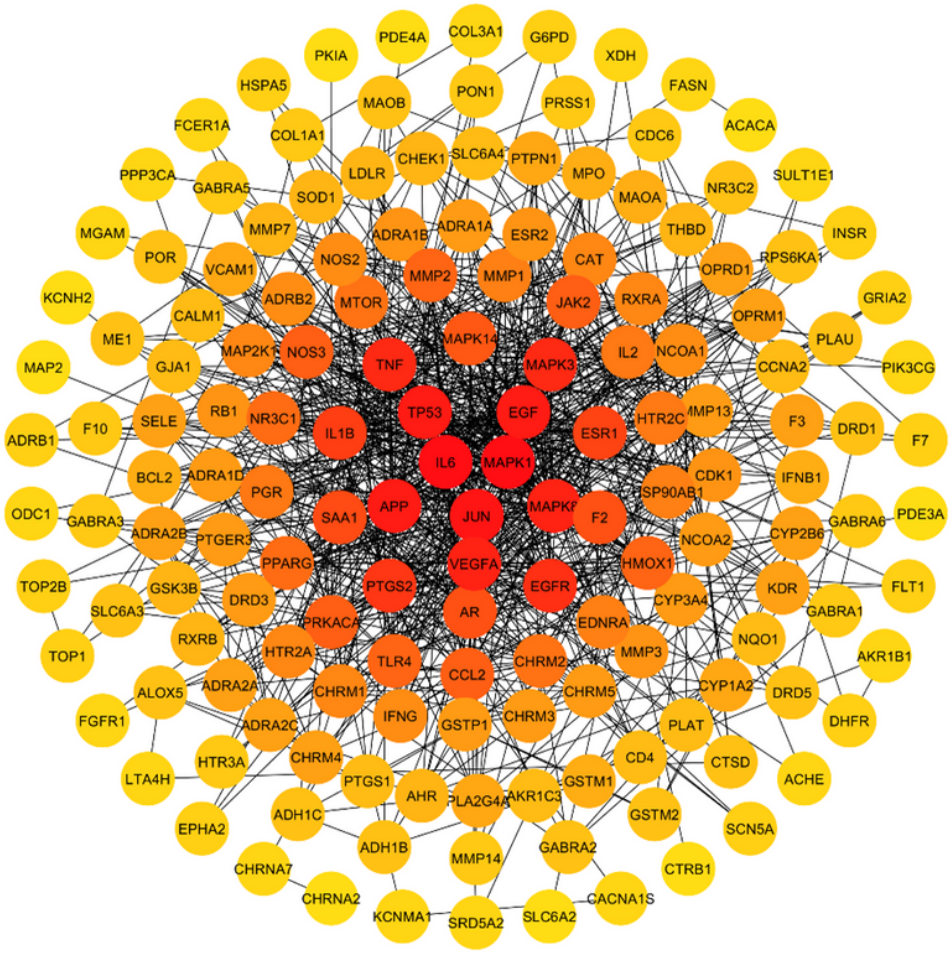

Figure 3

The PPI network map of target in ZSW for DN treatment. The spot represents the potential target of DN treatment. The darker spot closer to the center has higher degree value. Each black edge represents the interaction between the targets.

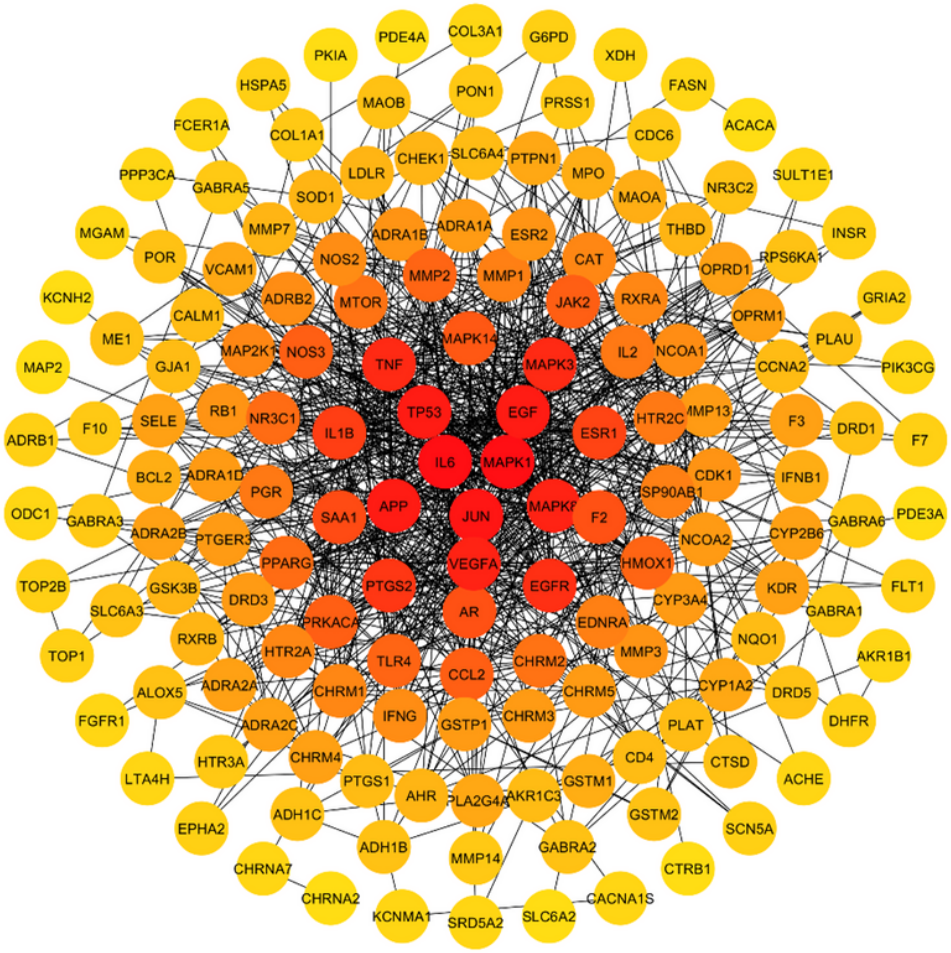

Figure 3

The PPI network map of target in ZSW for DN treatment. The spot represents the potential target of DN treatment. The darker spot closer to the center has higher degree value. Each black edge represents the interaction between the targets.

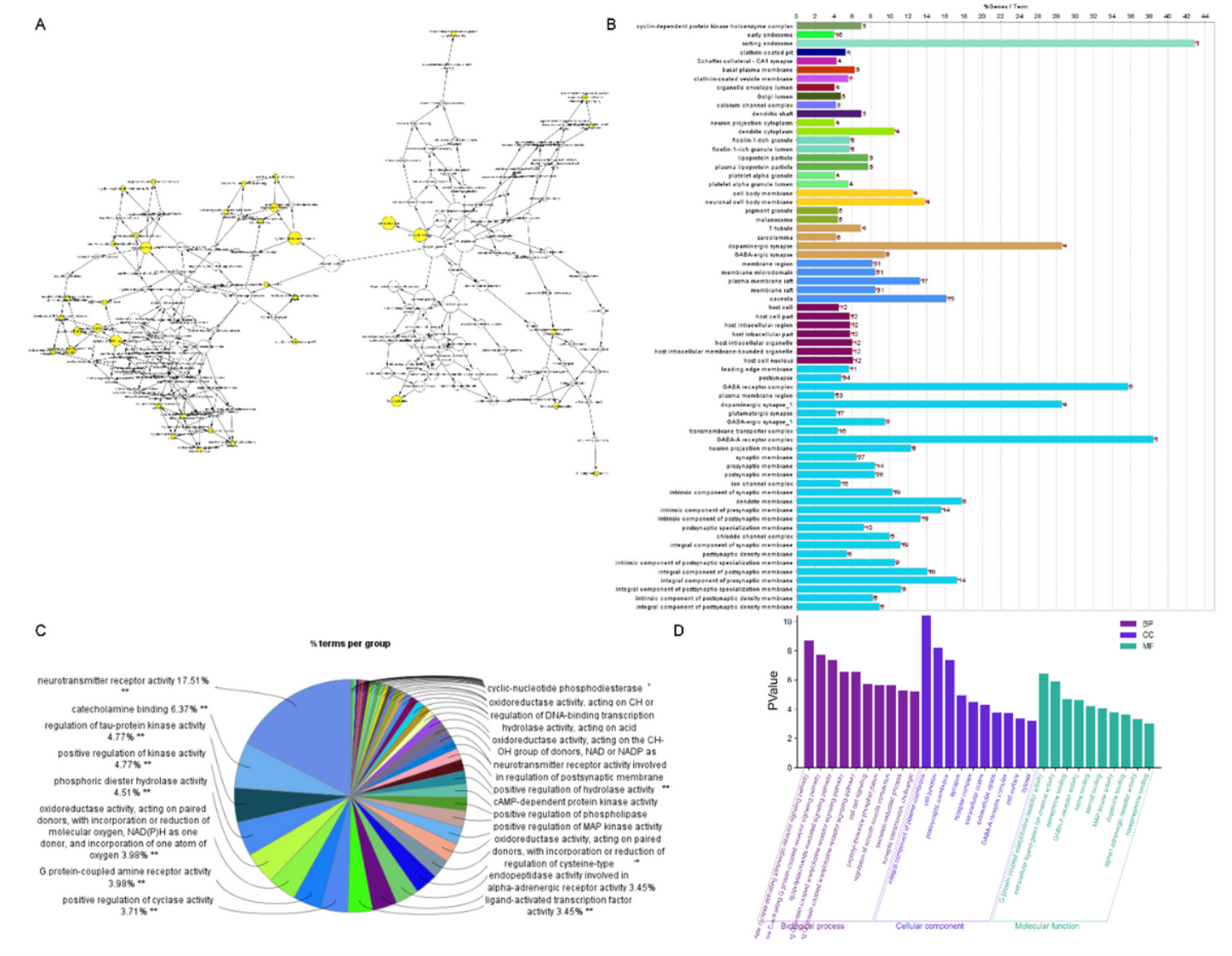

Figure 4

GO enrichment analysis of target in ZSW for DN treatment. A: GO biological process enrichment analysis; B: GO cell component enrichment analysis; C: GO molecular function enrichment analysis; D: The top 10 GO enrichment results.

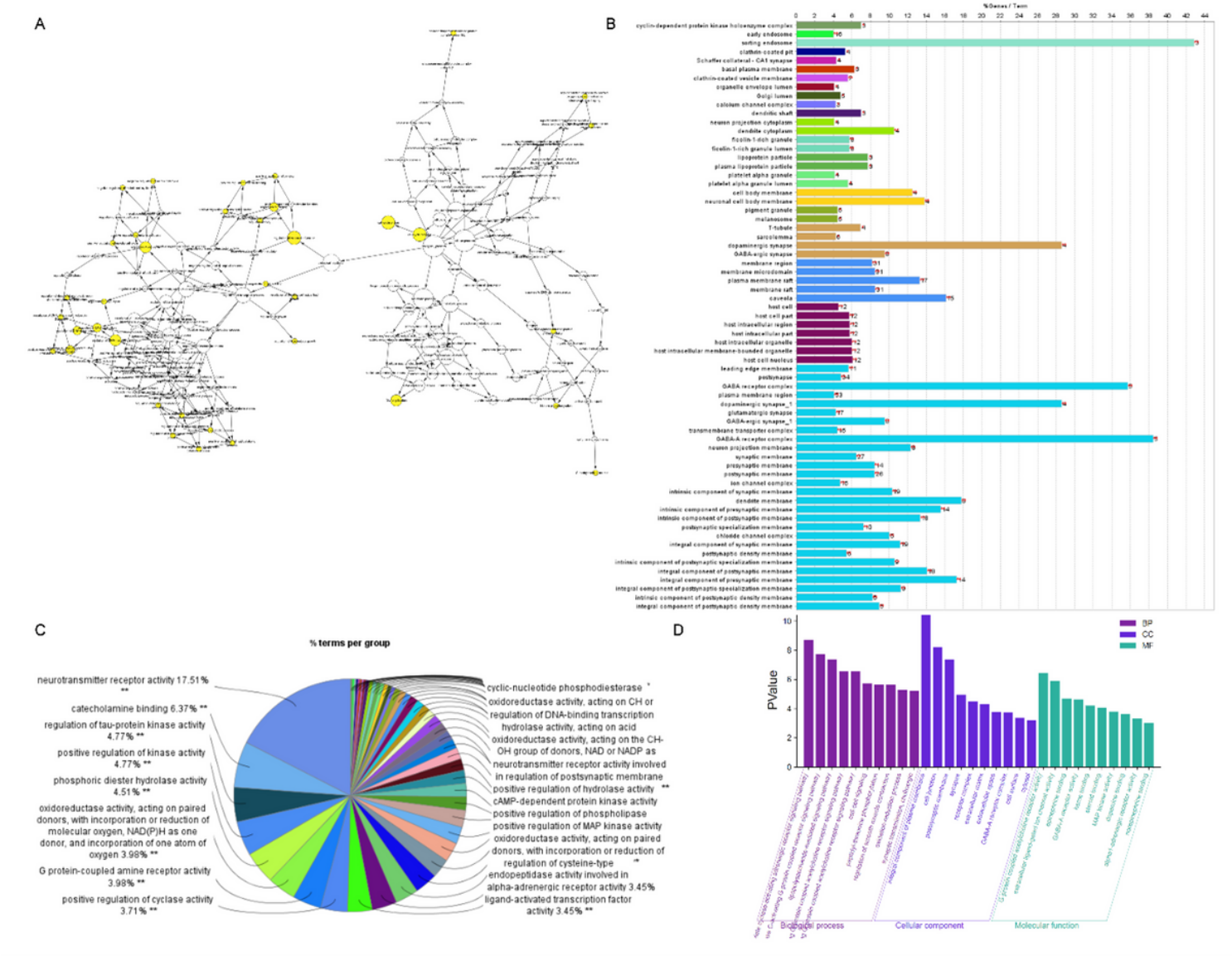

Figure 4

GO enrichment analysis of target in ZSW for DN treatment. A: GO biological process enrichment analysis; B: GO cell component enrichment analysis; C: GO molecular function enrichment analysis; D: The top 10 GO enrichment results.

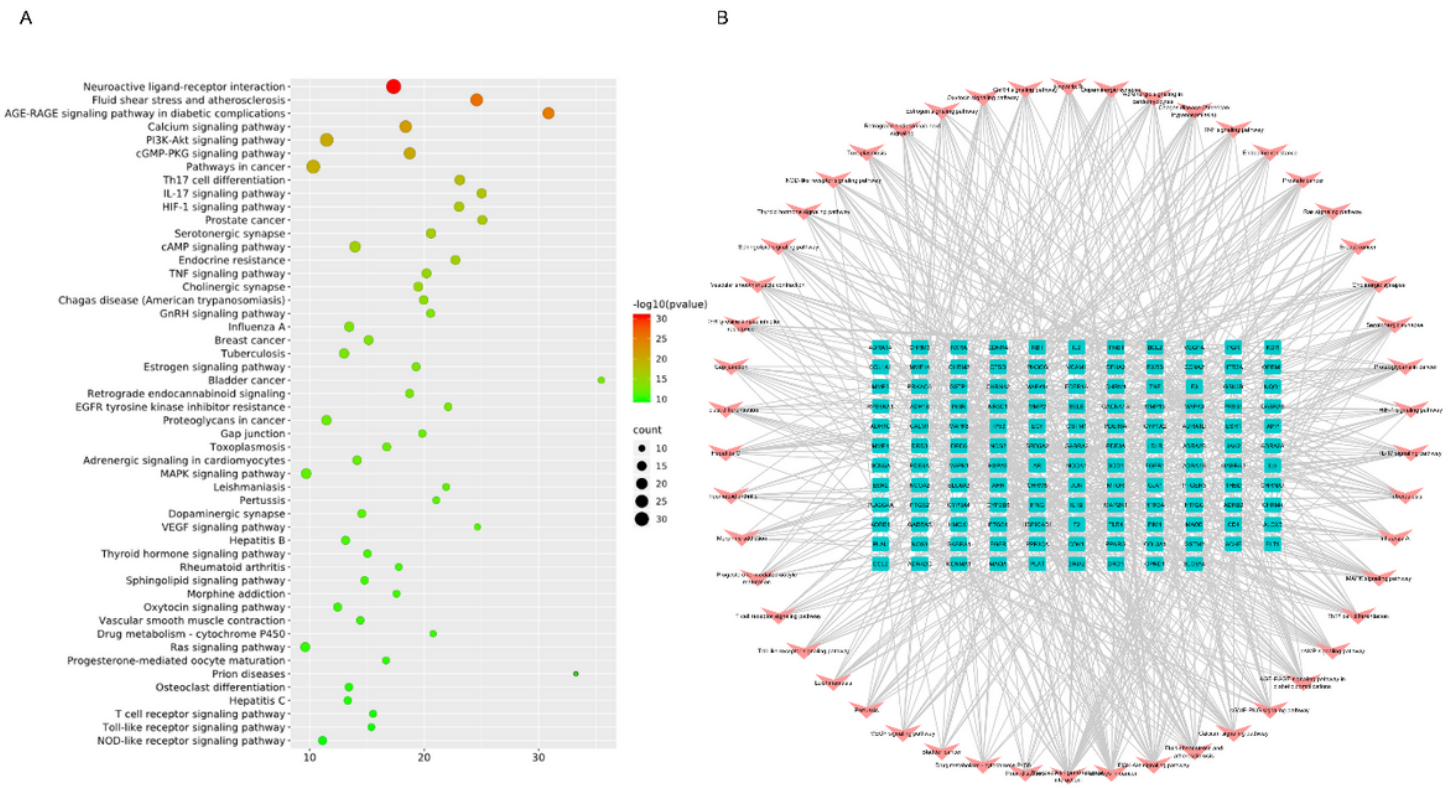

Figure 5

KEGG pathway enrichment analysis of target in ZSW for DN treatment. A: The enrichment results of the top 50 KEGG pathways. B: The “targets-top 50 pathways” network. The rose-red arrow represents the pathway. The green rectangle represents the potential target of DN treatment. Each gray edge represents the interaction between chemical ingredients and targets.

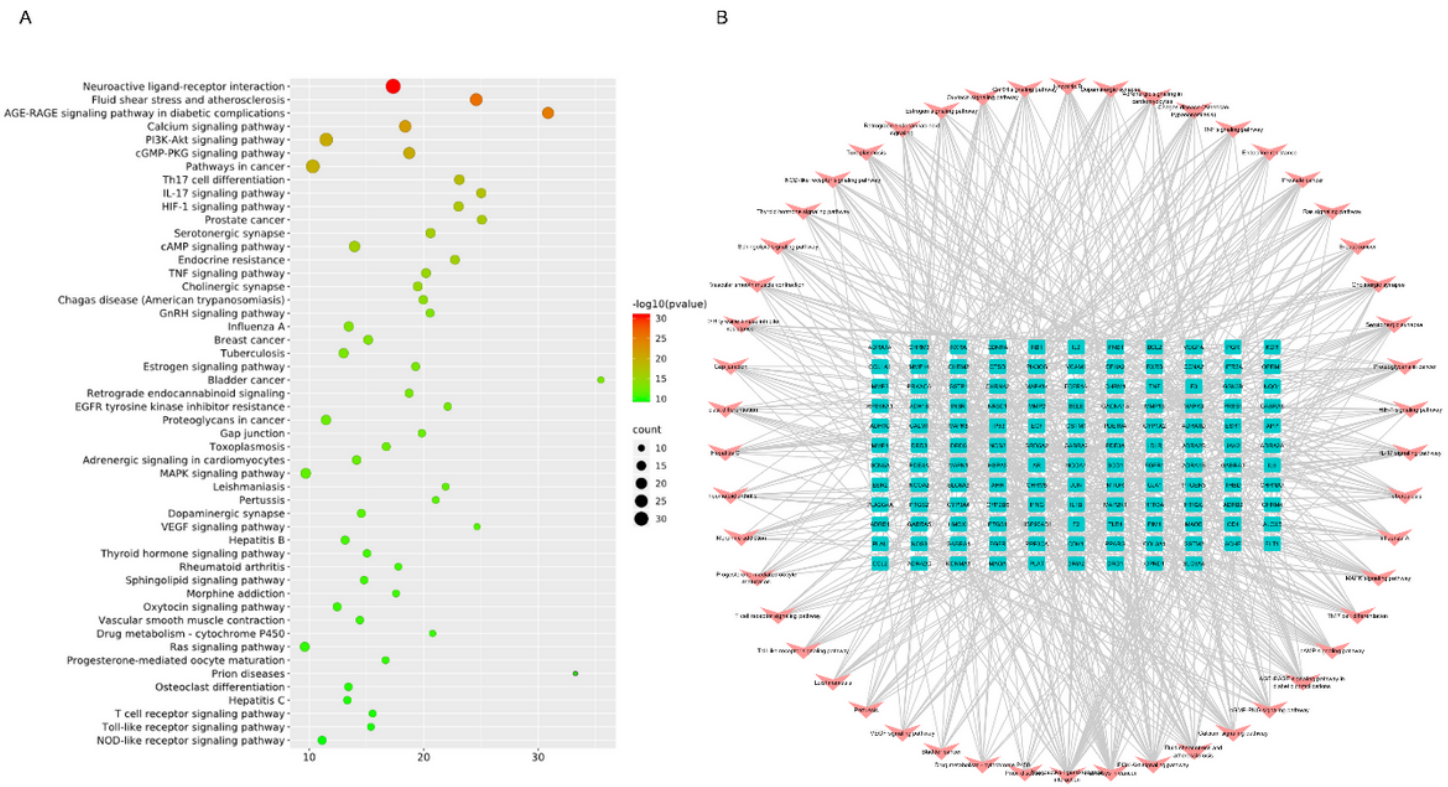

Figure 5

KEGG pathway enrichment analysis of target in ZSW for DN treatment. A: The enrichment results of the top 50 KEGG pathways. B: The “targets-top 50 pathways” network. The rose-red arrow represents the pathway. The green rectangle represents the potential target of DN treatment. Each gray edge represents the interaction between chemical ingredients and targets.

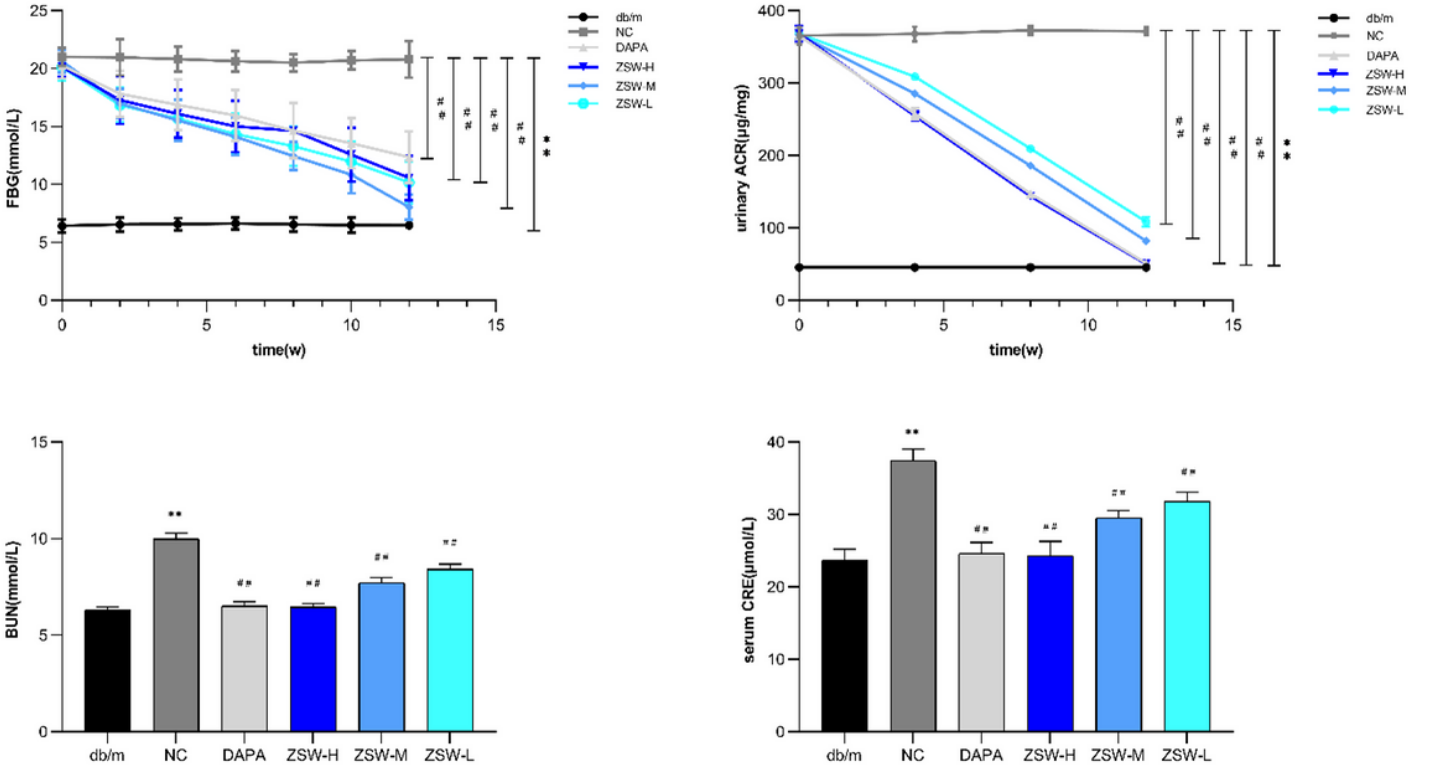

Figure 6

ZSW treatment alleviated the blood-sugar levels and the major biochemical indexes of renal injuries detected in db/db mice. The values were presented as mean ± standard error of mean. **P < 0.01, vs db/m group; ##P < 0.01, vs NC group. DAPA: dapagliflozin (1.0mg/kg); NC: normal control; ZSW-H: high dose ZSW (6.0mg/kg); ZSW-L: low dose ZSW (3.0mg/kg); ZSW-M: medium dose ZSW (1.5mg/kg).

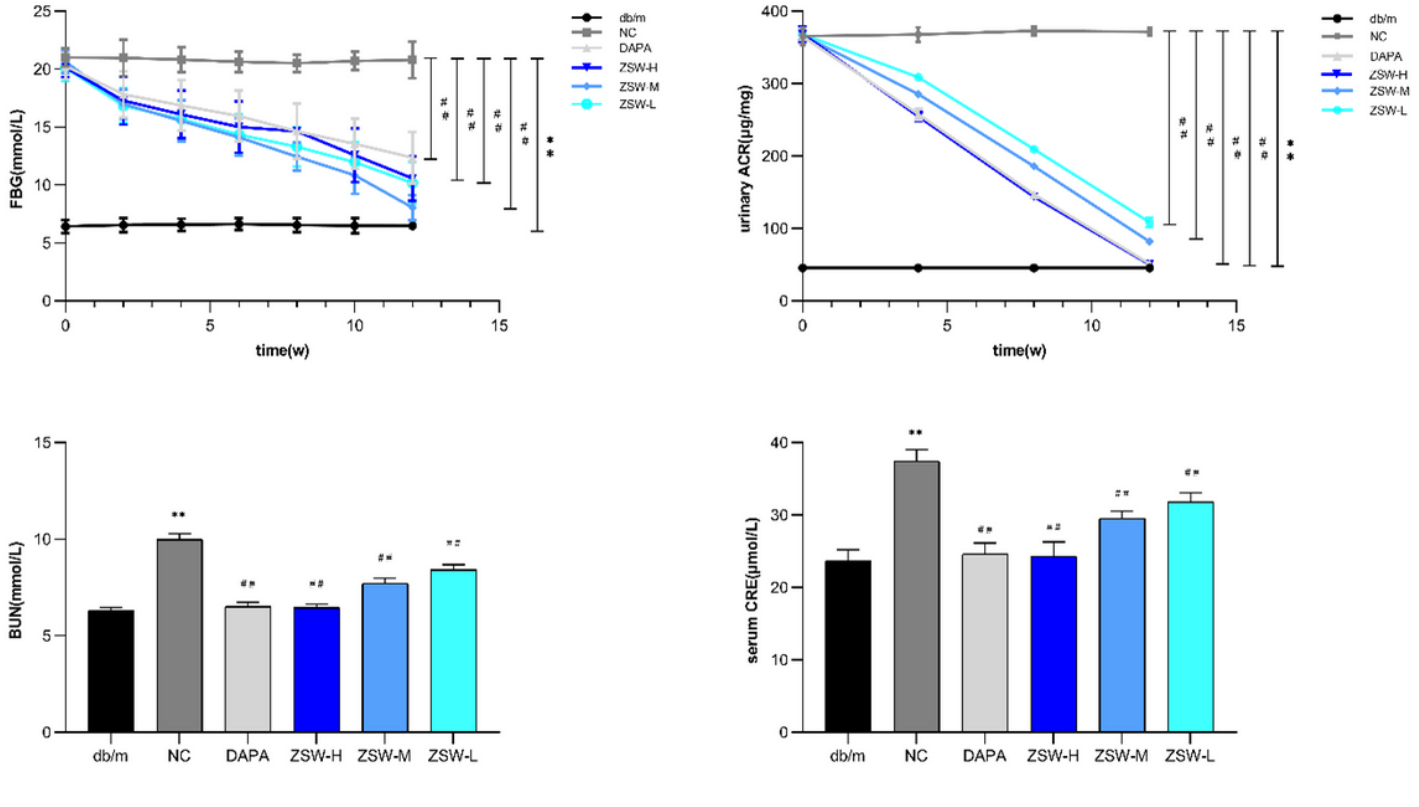

Figure 6

ZSW treatment alleviated the blood-sugar levels and the major biochemical indexes of renal injuries detected in db/db mice. The values were presented as mean ± standard error of mean. **P < 0.01, vs db/m group; ##P < 0.01, vs NC group. DAPA: dapagliflozin (1.0mg/kg); NC: normal control; ZSW-H: high dose ZSW (6.0mg/kg); ZSW-L: low dose ZSW (3.0mg/kg); ZSW-M: medium dose ZSW (1.5mg/kg).

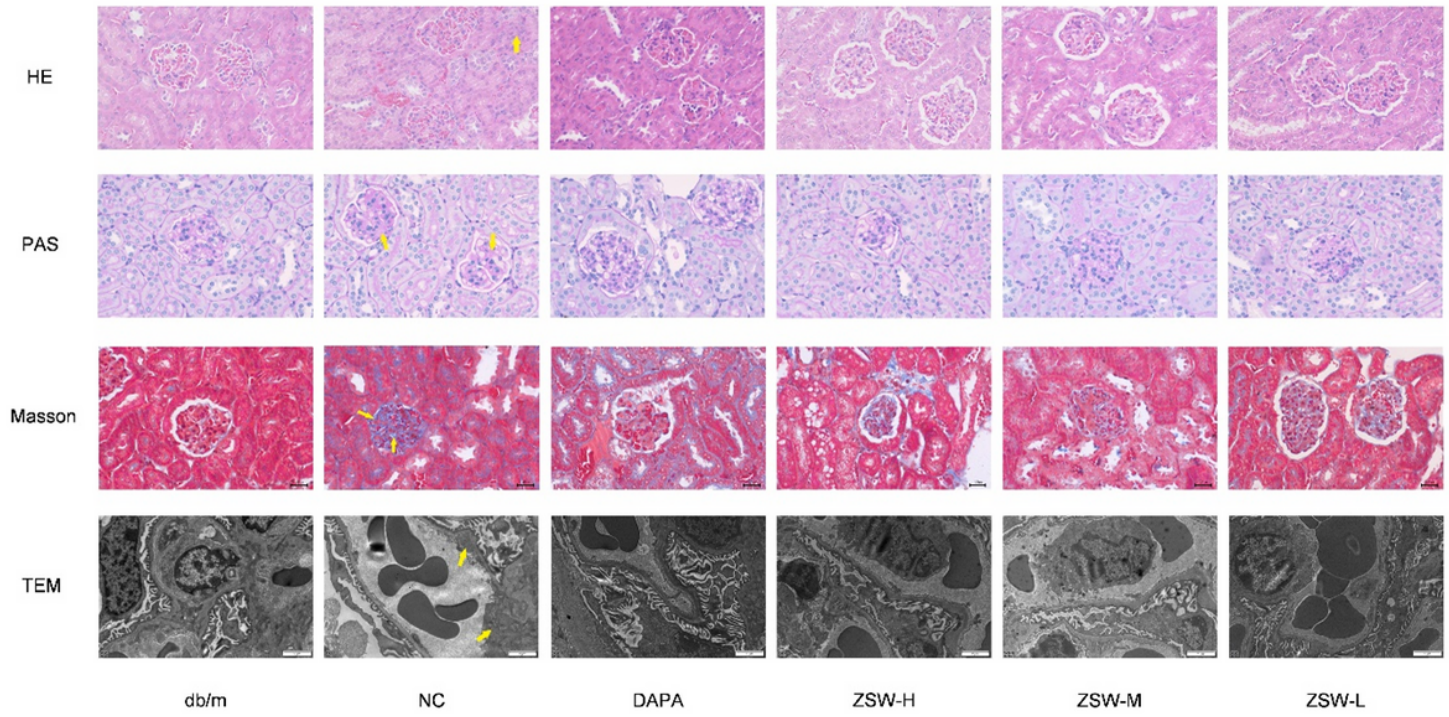

Figure 7

ZSW and DAPA treatment alleviated renal injuries detected by light microscopy (HE, PAS, and Masson staining, 400×) and TEM (6000×) in renal tissues of db/db mice. GBM thickening (shown in Masson staining and TEM), mesangial matrix expansion (shown in PAS staining and TEM) and tubular inflammation (shown in HE staining) were indicated by yellow arrows. DAPA: dapagliflozin (1.0mg/kg); NC: normal control; ZSW-H: high dose ZSW (6.0mg/kg); ZSW-L: low dose ZSW (3.0mg/kg); ZSW-M: medium dose ZSW (1.5mg/kg).

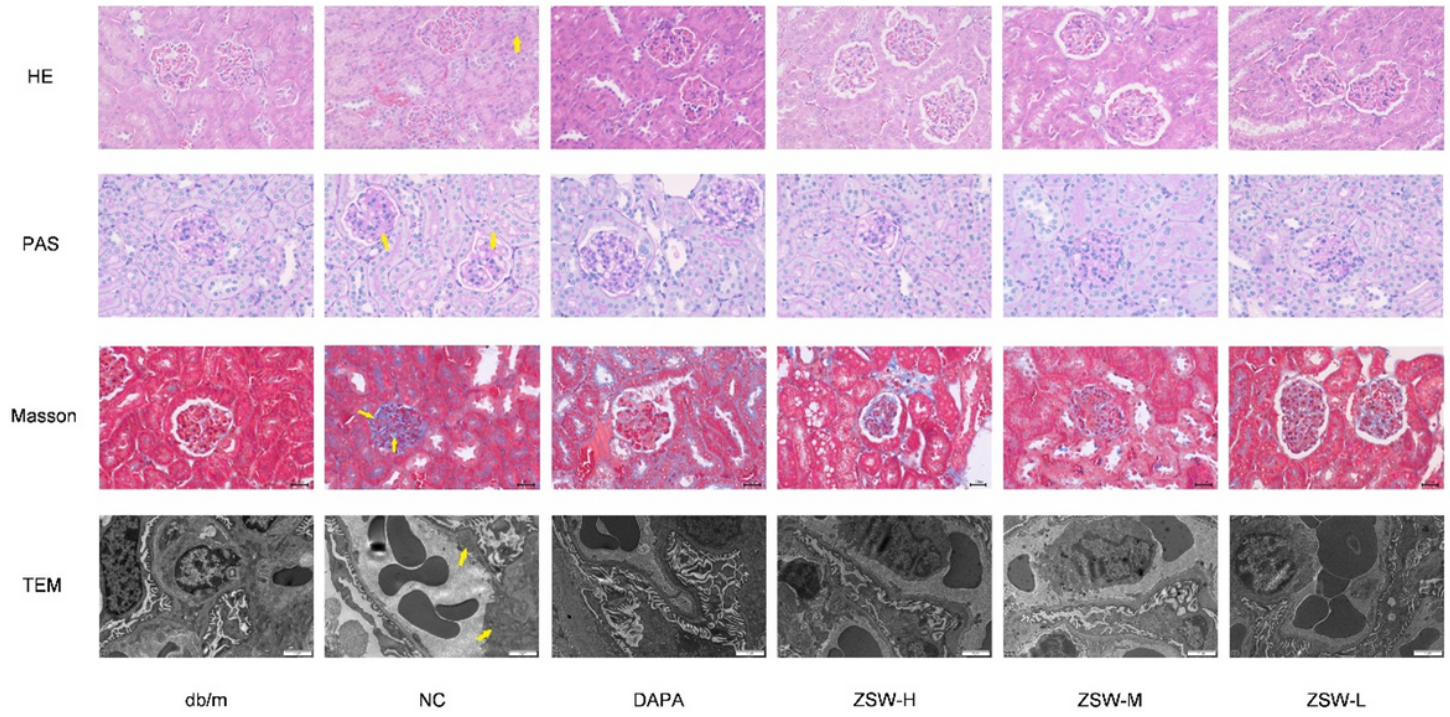

Figure 7

ZSW and DAPA treatment alleviated renal injuries detected by light microscopy (HE, PAS, and Masson staining, 400×) and TEM (6000×) in renal tissues of db/db mice. GBM thickening (shown in Masson staining and TEM), mesangial matrix expansion (shown in PAS staining and TEM) and tubular inflammation (shown in HE staining) were indicated by yellow arrows. DAPA: dapagliflozin (1.0mg/kg); NC: normal control; ZSW-H: high dose ZSW (6.0mg/kg); ZSW-L: low dose ZSW (3.0mg/kg); ZSW-M: medium dose ZSW (1.5mg/kg).

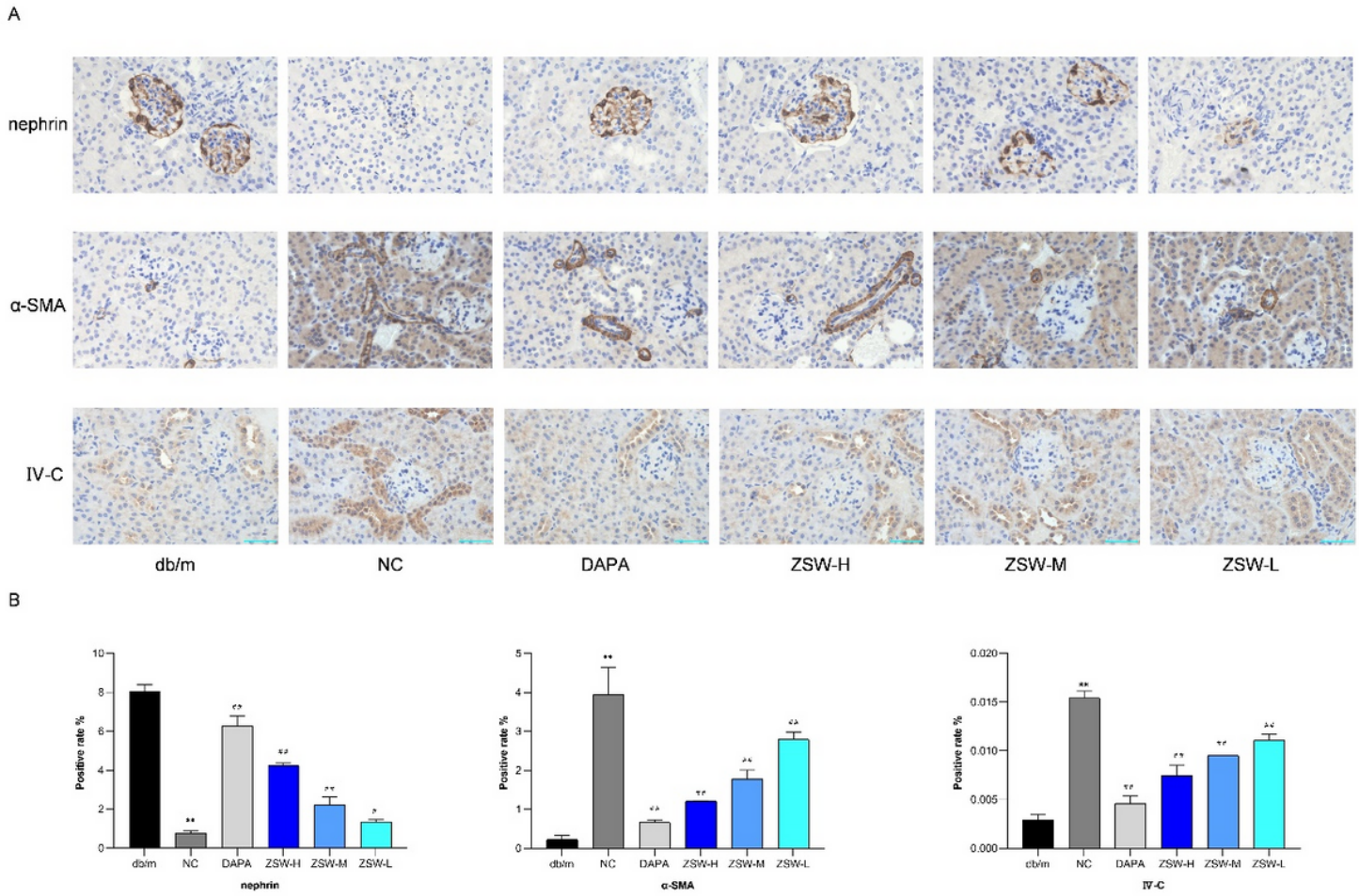

Figure 8

ZSW and DAPA treatment regulated the major biomarkers of renal injuries in db/db mice. A: Nephrin, α-SMA and IV-C expression detected by IHC analysis; B: The positive rate of the IHC results. The values were presented as mean ± standard error of mean. **P < 0.01, vs db/m group; #P < 0.05, ##P < 0.01, vs NC group. DAPA: dapagliflozin (1.0mg/kg); NC: normal control; ZSW-H: high dose ZSW (6.0mg/kg); ZSW-L: low dose ZSW (3.0mg/kg); ZSW-M: medium dose ZSW (1.5mg/kg).

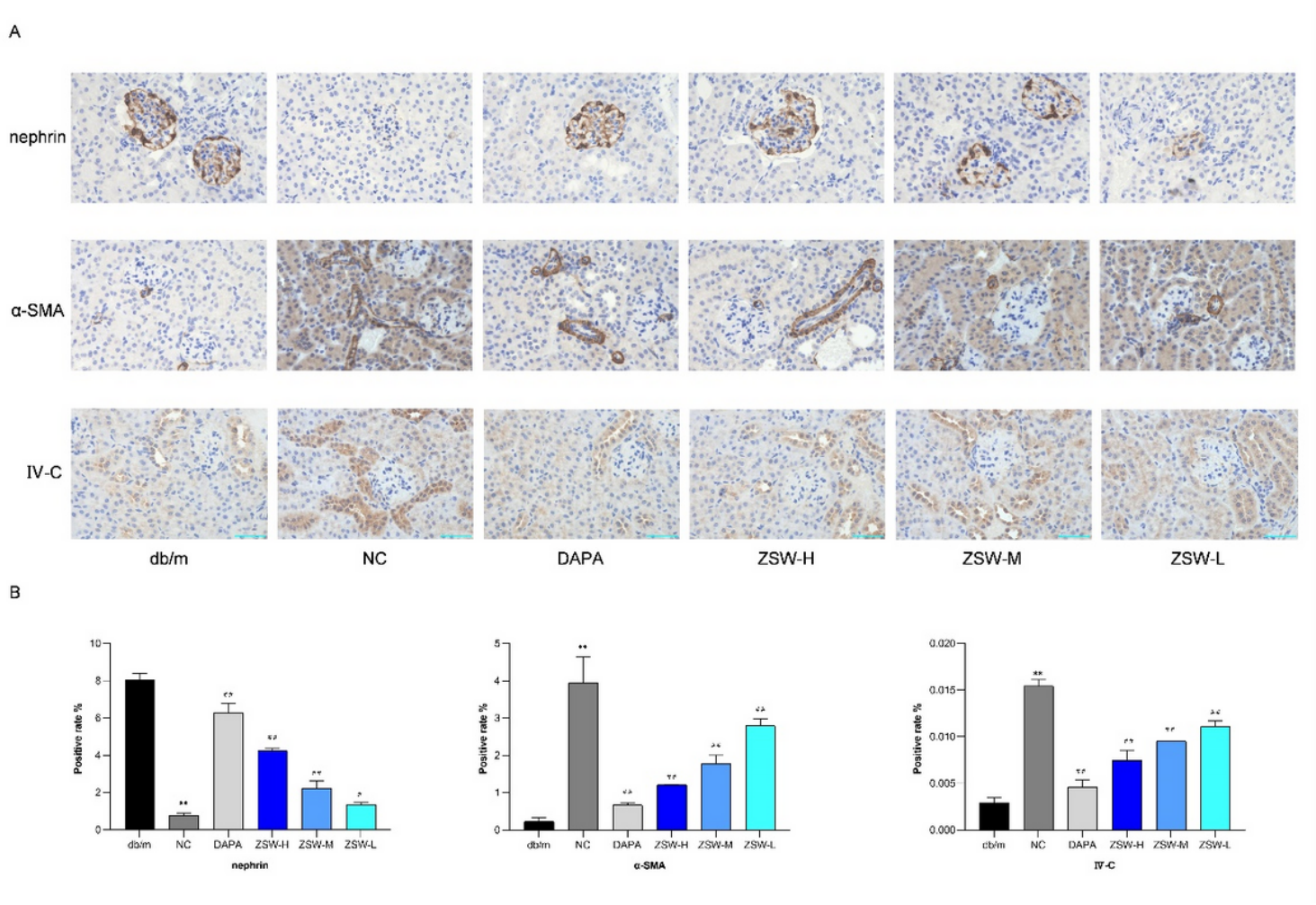

Figure 8

ZSW and DAPA treatment regulated the major biomarkers of renal injuries in db/db mice. A: Nephrin, α-SMA and IV-C expression detected by IHC analysis; B: The positive rate of the IHC results. The values were presented as mean ± standard error of mean. **P < 0.01, vs db/m group; #P < 0.05, ##P < 0.01, vs NC group. DAPA: dapagliflozin (1.0mg/kg); NC: normal control; ZSW-H: high dose ZSW (6.0mg/kg); ZSW-L: low dose ZSW (3.0mg/kg); ZSW-M: medium dose ZSW (1.5mg/kg).

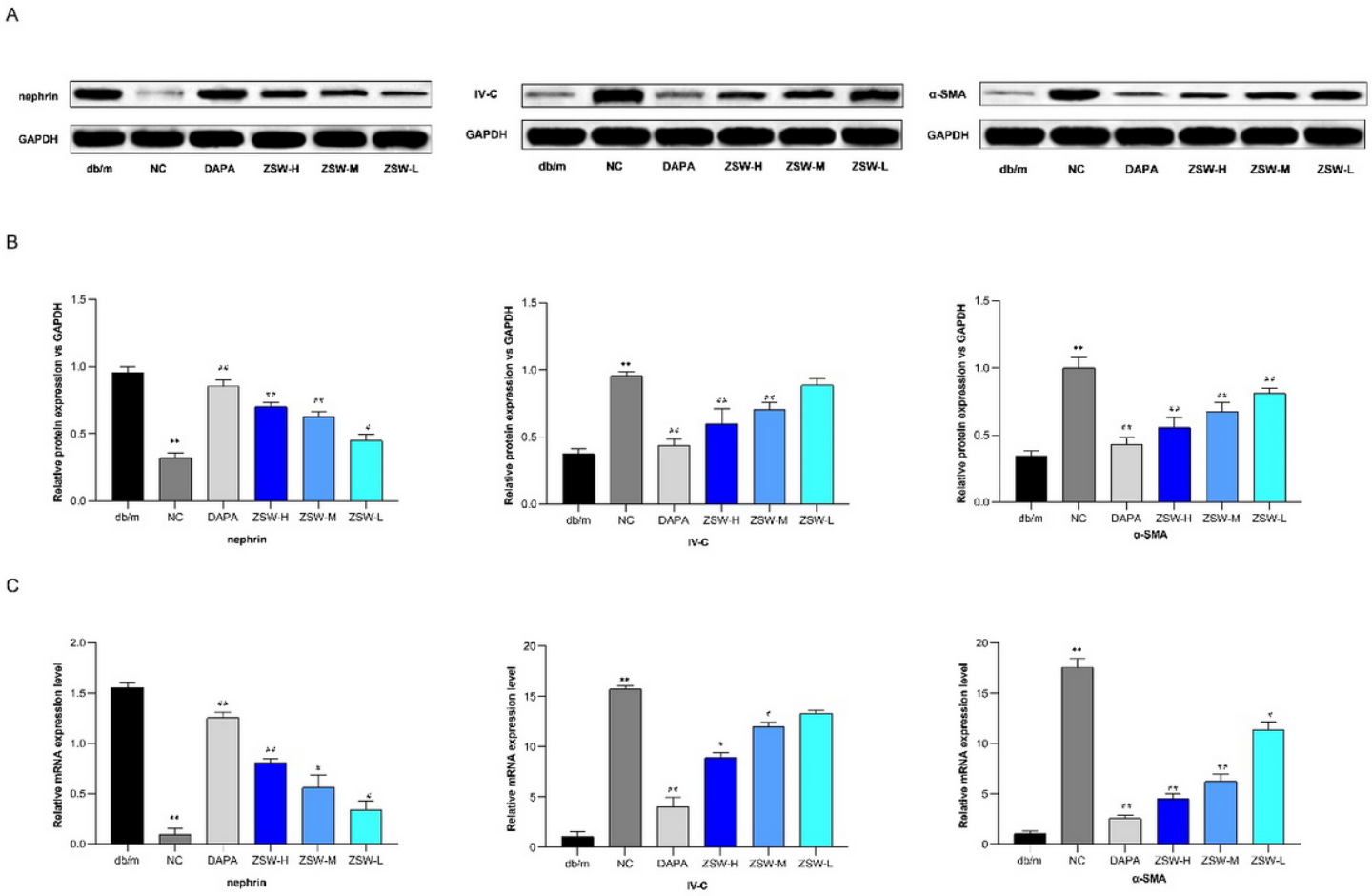

Figure 9

ZSW and DAPA treatment regulated protein and mRNA expressions of nephrin, α-SMA and IV-C in db/db mice. A: The levels of nephrin, α-SMA and IV-C protein detected by WB. B: The relative protein levels of the WB results; C: The levels of nephrin, α-SMA and IV-C mRNA assessed by RT-qPCR. The values were presented as mean ± standard error of mean. **P < 0.01, vs db/m group; #P < 0.05, ##P < 0.01, vs NC group. DAPA: dapagliflozin (1.0mg/kg); NC: normal control; ZSW-H: high dose ZSW (6.0mg/kg); ZSW-L: low dose ZSW (3.0mg/kg); ZSW-M: medium dose ZSW (1.5mg/kg).

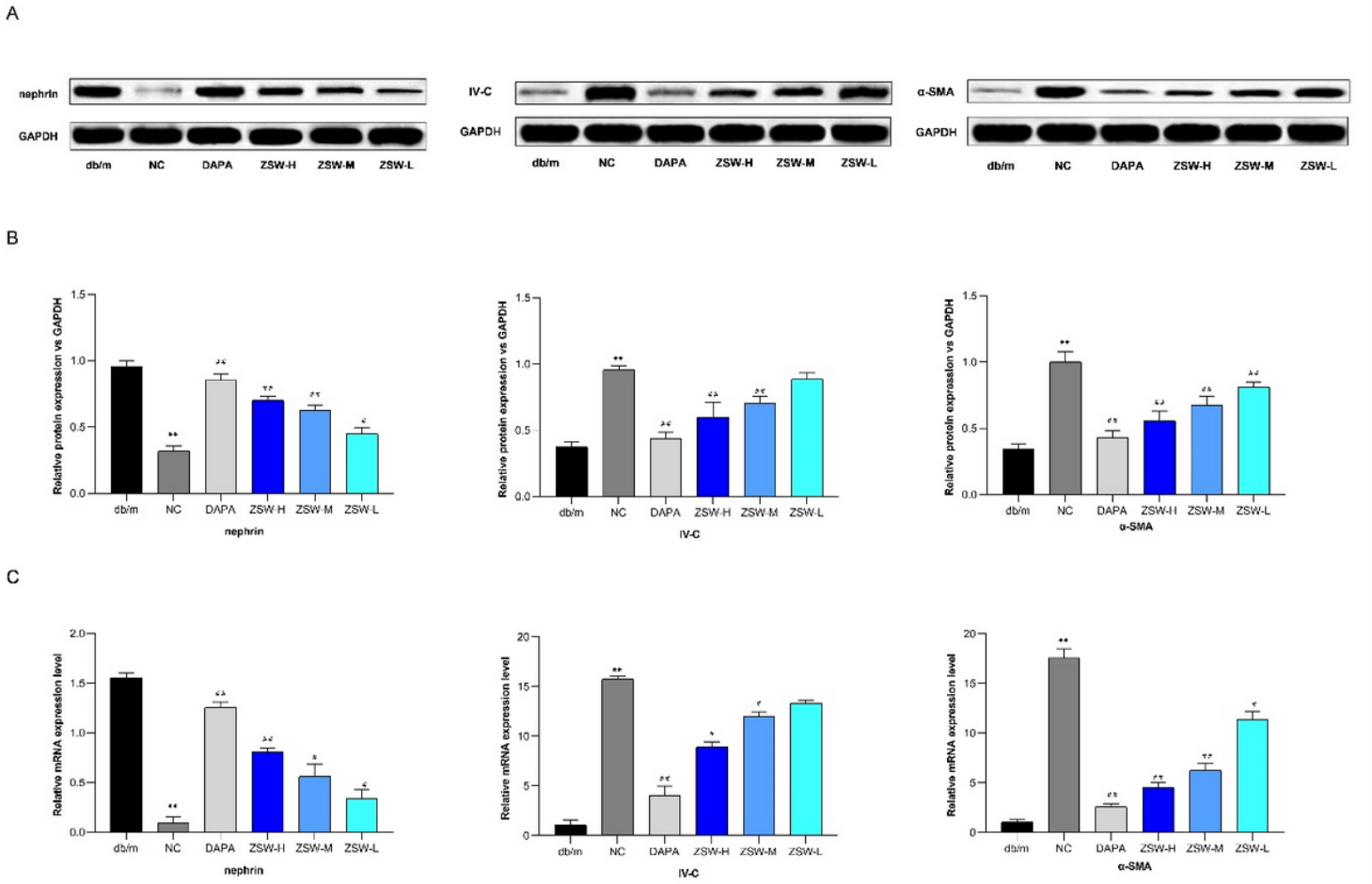

Figure 9

ZSW and DAPA treatment regulated protein and mRNA expressions of nephrin, α-SMA and IV-C in db/db mice. A: The levels of nephrin, α-SMA and IV-C protein detected by WB. B: The relative protein levels of the WB results; C: The levels of nephrin, α-SMA and IV-C mRNA assessed by RT-qPCR. The values were presented as mean ± standard error of mean. **P < 0.01, vs db/m group; #P < 0.05, ##P < 0.01, vs NC group. DAPA: dapagliflozin (1.0mg/kg); NC: normal control; ZSW-H: high dose ZSW (6.0mg/kg); ZSW-L: low dose ZSW (3.0mg/kg); ZSW-M: medium dose ZSW (1.5mg/kg).

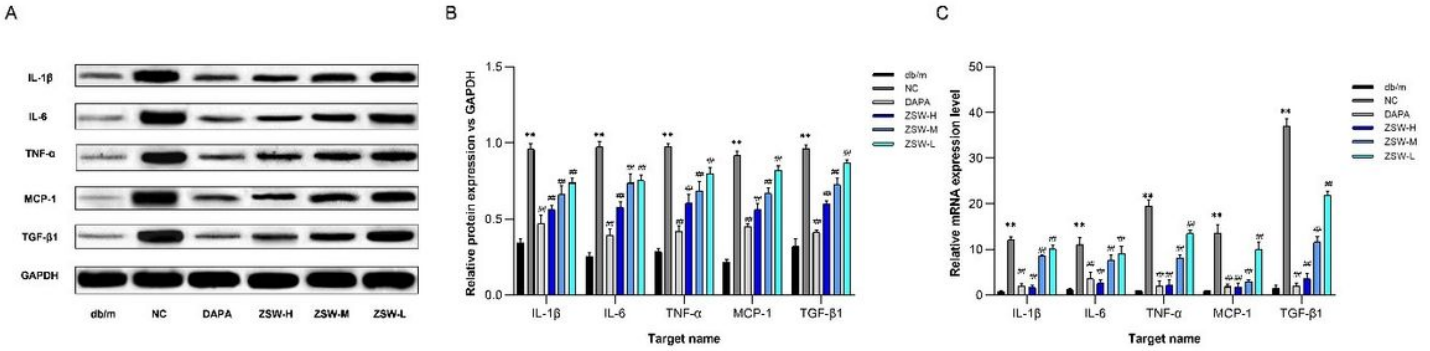

Figure 10

ZSW and DAPA treatment inhibited expression of multiple proinflammatory cytokines exaggerated in db/db mice. A: The levels of IL-1β, IL-6, TNF-α, MCP-1 and TGF-β1 protein detected by WB. B: The relative protein levels of the WB results; C: The levels of IL-1β, IL-6, TNF-α, MCP-1 and TGF-β1 mRNA assessed by RT-qPCR. The values were presented as mean ± standard error of mean. **P < 0.01, vs db/m group; ##P < 0.01, vs NC group. DAPA: dapagliflozin (1.0mg/kg); NC: normal control; ZSW-H: high dose ZSW (6.0mg/kg); ZSW-L: low dose ZSW (3.0mg/kg); ZSW-M: medium dose ZSW (1.5mg/kg).

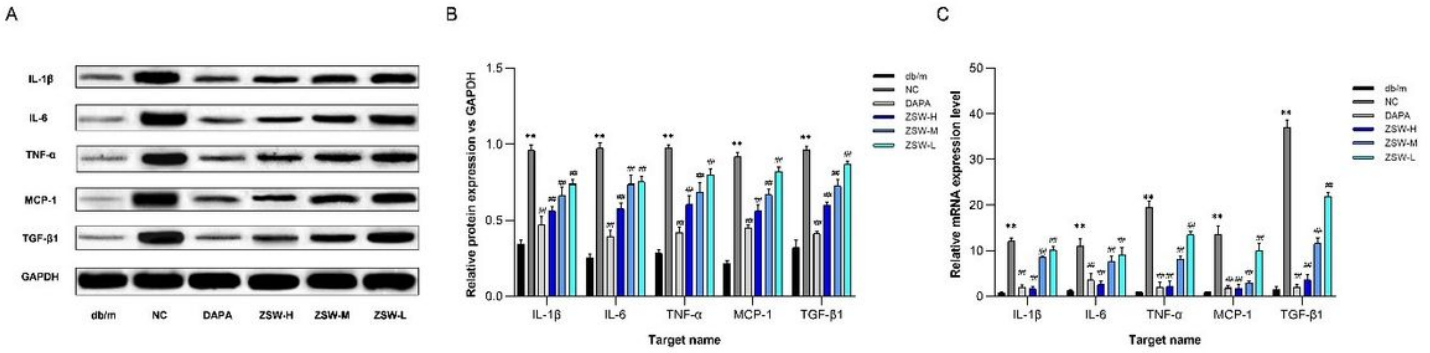

Figure 10

ZSW and DAPA treatment inhibited expression of multiple proinflammatory cytokines exaggerated in db/db mice. A: The levels of IL-1β, IL-6, TNF-α, MCP-1 and TGF-β1 protein detected by WB. B: The relative protein levels of the WB results; C: The levels of IL-1β, IL-6, TNF-α, MCP-1 and TGF-β1 mRNA assessed by RT-qPCR. The values were presented as mean ± standard error of mean. **P < 0.01, vs db/m group; ##P < 0.01, vs NC group. DAPA: dapagliflozin (1.0mg/kg); NC: normal control; ZSW-H: high dose ZSW (6.0mg/kg); ZSW-L: low dose ZSW (3.0mg/kg); ZSW-M: medium dose ZSW (1.5mg/kg).

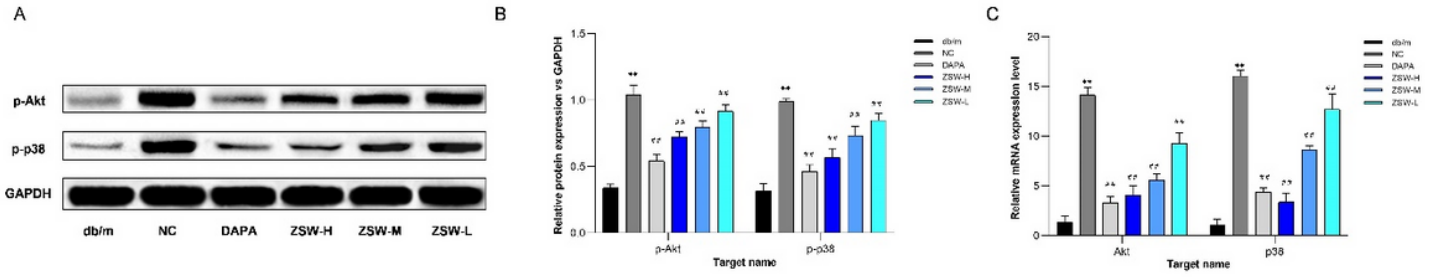

Figure 11

ZSW and DAPA treatment regulated the expression of key nodes in P13K/Akt and p38 MAPK signaling pathway activated in db/db mice. A: The levels of p-Akt and p-p38 protein detected by WB. B: The relative protein levels of the WB results; C: The levels of Akt and p38 MAPK mRNA assessed by RT-qPCR. The values were presented as mean ± standard error of mean. **P < 0.01, vs db/m group; ##P < 0.01, vs NC group. DAPA: dapagliflozin (1.0mg/kg); NC: normal control; ZSW-H: high dose ZSW (6.0mg/kg); ZSW-L: low dose ZSW (3.0mg/kg); ZSW-M: medium dose ZSW (1.5mg/kg).

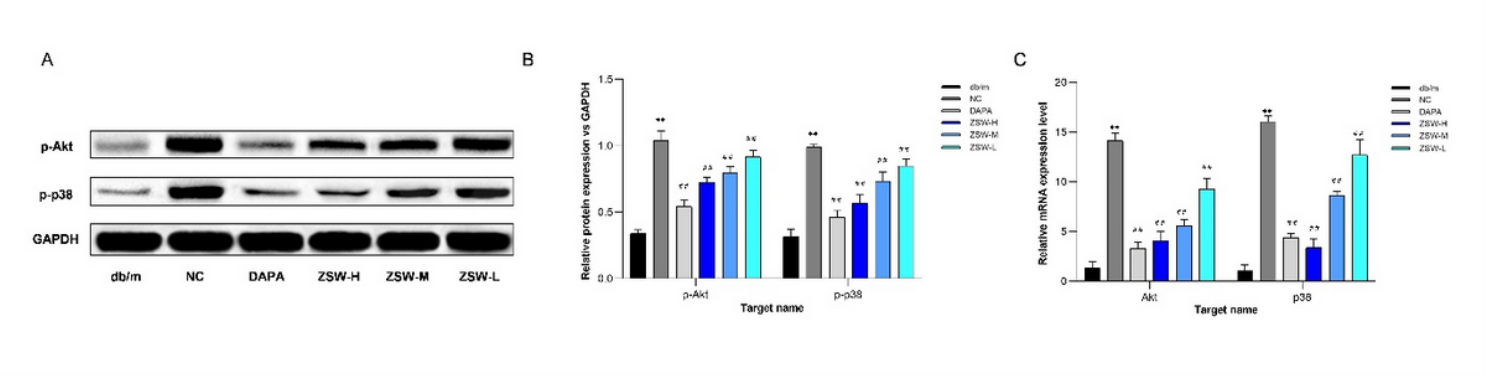

Figure 11

ZSW and DAPA treatment regulated the expression of key nodes in P13K/Akt and p38 MAPK signaling pathway activated in db/db mice. A: The levels of p-Akt and p-p38 protein detected by WB. B: The relative protein levels of the WB results; C: The levels of Akt and p38 MAPK mRNA assessed by RT-qPCR. The values were presented as mean ± standard error of mean. **P < 0.01, vs db/m group; ##P < 0.01, vs NC group. DAPA: dapagliflozin (1.0mg/kg); NC: normal control; ZSW-H: high dose ZSW (6.0mg/kg); ZSW-L: low dose ZSW (3.0mg/kg); ZSW-M: medium dose ZSW (1.5mg/kg).